Orchestrated activation of mGluR5 and CB$_1$ promotes neuroprotection

Edleusa M. L. Batista[1], Juliana G. Doria[1], Talita H. Ferreira-Vieira[1], Juliana Alves-Silva[1], Stephen S. G. Ferguson[2], Fabricio A. Moreira[3] and Fabiola M. Ribeiro[1*]

Abstract

The metabotropic glutamate receptor 5 (mGluR5) and the cannabinoid receptor 1 (CB$_1$) exhibit a functional interaction, as CB$_1$ regulates pre-synaptic glutamate release and mGluR5 activation increases endocannabinoid synthesis at the post-synaptic site. Since both mGluR5 and CB$_1$ promote neuroprotection, we delineated experiments to investigate a possible link between CB$_1$ and mGluR5 activation in the induction of neuroprotection using primary cultured corticostriatal neurons. We find that either the pharmacological blockade or the genetic ablation of either mGluR5 or CB$_1$ can abrogate both CB$_1$- and mGluR5-mediated neuroprotection against glutamate insult. Interestingly, decreased glutamate release and diminished intracellular Ca^{2+} do not appear to play a role in CB$_1$ and mGluR5-mediated neuroprotection. Rather, these two receptors work cooperatively to trigger the activation of cell signaling pathways to promote neuronal survival, which involves MEK/ERK1/2 and PI3K/AKT activation. Interestingly, although mGluR5 activation protects postsynaptic terminals and CB$_1$ the presynaptic site, intact signaling of both receptors is required to effectively promote neuronal survival. In conclusion, mGluR5 and CB$_1$ act in concert to activate neuroprotective cell signaling pathways and promote neuronal survival.

Keywords: mGluR5, CB1, Cell death, AKT, ERK1/2

Abbreviations: 2-AG, 2-arachidonoylglycerol; ACEA, Arachidonyl-2'-Chloroethylamide; AM, Acetoxymethyl Ester; AM251, 1-(2,4-Dichlorophenyl)-5-(4-iodophenyl)-4-methyl-N-1-piperidinyl-1H-pyrazole-3-carboxamide; anandamide, N-arachidonoylethanolamine; APP, Amyloid Precursor Protein; Aβ, Amyloid-β Peptide; BDNF, Brain Derived Neurotrophic Factor; CB$_1$, Cannabinoid Receptor 1; CDPPB, 3-cyano-*N*-(1,3-diphenyl-1*H*-pyrazol-5-yl) benzamide; DAG, Diacylglycerol; DGL-α, Diacylglycerol Lipase-α; DIV, Days In Vitro; ERK, Extracellular-Signal-Regulated Kinase; FAAH, Fatty Acid Amide Hydrolase; GABA, Gamma-Aminobutyric Acid; GPCR, G-protein Coupled Receptor; HBSS, Hank's Balanced Salt Solution; HD, Huntington's Disease; IP$_3$, Inositol-1,4,5-triphosphate; JZL184, 4-[Bis(1,3-benzodioxol-5-yl)-hydroxymethyl]piperidine-1-carboxylate 4-nitrophenyl ester; LTD, Long Term Depression; LY294002, 2-(4-morpholinyl)-8-phenyl-1(4H)-benzopyran-4-one hydrochloride; MEK, Mitogen-Activated Protein Kinase Kinase; MGL, Monoacylglycerol Lipase; mGluR5, Metabotropic Glutamate Receptor 5; MPEP, 2-methyl-6-(phenylethynyl)-pyridine; NC, Negative Control; PAM, Positive Allosteric Modulator; PD98059, 2-(2-amino-3-methoxyphenyl)-4h-1-benzopyran-4-one; PDK1, Phosphoinositide-Dependent Kinase; PI3K, Phosphatidylinositol-3 kinase; PIKE, PI3K Enhancer; PLC, Phospholipase C; PSD95, Postsynaptic Density Protein; Pyk2, Proline-Rich Tyrosine Kinase 2; siRNA, Small Interfering RNA; URB597, Cyclohexyl Carbamic Acid 3'-carbamoyl-biphenyl-3-yl ester; Δ^9-THC, Δ^9-tetrahydrocannabinol

* Correspondence: fmribeiro@icb.ufmg.br
[1]Departamento de Bioquimica e Imunologia, Instituto de Ciencias Biologicas, Universidade Federal de Minas Gerais, Ave. Antonio Carlos 6627, Belo Horizonte, MG CEP: 31270-901, Brazil
Full list of author information is available at the end of the article

Batista *et al. Molecular Brain* (2016) 9:80

Page 2 of 17

Introduction

The metabotropic glutamate receptor 5 (mGluR5) is a G-protein coupled receptor (GPCR) that is present at the postsynaptic site and is involved in a wide variety of processes, including motor behaviour, nociception, memory and neurodegeneration [1, 10, 12, 18, 22, 53]. mGluR5 stimulation promotes activation of $G\alpha_{q/11}$ proteins, which trigger the activation of phospholipase Cβ1 (PLCβ1), leading to diacylglycerol (DAG) and inositol-1,4,5-triphosphate (IP$_3$) formation and the release of Ca^{2+} from intracellular stores. In addition, most likely by coupling to homer proteins, mGluR5 also activates other cell signaling pathways, including extracellular-signal-regulated kinase 1/2 (ERK1/2) and AKT [7, 10, 21, 35, 48, 50]. We have recently demonstrated that mGluR5 positive allosteric modulators (PAMs) preferentially activate neuroprotective cell signaling pathways and prevent neuronal cell death in primary cultured striatal neurons, as well as in a mouse model of Huntington's disease (HD) [10, 11]. Importantly, the memory loss observed in this mouse model of HD can be rescued by the treatment with the mGluR5 PAM, CDPPB [10].

Activation of the endocannabinoid system also mediates neuroprotection [2, 36, 52]. Δ^9-tetrahydrocannabinol (Δ^9-THC), the main active component of the plant *Cannabis sativa*, as well as endocannabinoids, including anandamide and 2-arachidonoylglycerol (2-AG), activate cannabinoid receptor 1 (CB$_1$), which is a $G\alpha_{i/o}$–coupled receptor mainly found at the presynaptic terminal. Endocannabinoids are synthesized on demand at the post-synaptic terminal and act on cannabinoid receptors to prevent the release of neurotransmitters, including gamma-aminobutyric acid (GABA) and glutamate [26, 44, 66]. Therefore, CB$_1$ can diminish excitotoxic neurotransmission by lessening pre-synaptic glutamate release [28, 36]. Similarly to mGluR5, CB$_1$ activation stimulates neuroprotective ERK1/2 and AKT cell signaling pathways, which are involved in the control of cell survival [4, 15, 63, 65].

Previous studies have demonstrated that mGluR5 and CB$_1$ exhibit a functional interaction that is implicated in a wide variety of processes, including pain [47], cocaine addiction [13], Fragile X syndrome [57], anxiety and memory [62]. Interestingly, activation of mGluR5 stimulates endocannabinoid synthesis by increasing intracellular Ca^{2+} [6]. However, mGluR5 can also increase 2-AG synthesis in a mechanism that is independent of Ca^{2+} [45]. Homer proteins, which bind to mGluR5, also bind to the two key proteins responsible for 2-AG synthesis, PLCβ, which is activated by mGluR5, and diacylglycerol lipase-α (DGL-α) [23, 25]. The formation of this protein complex enables the rapid formation of 2-AG following mGluR5 stimulation. At the same time, by activating pre-synaptic CB$_1$, 2AG blunts glutamate release and as a

consequence mGluR5 activation [36, 52]. However, it is still not known whether these two receptors could function cooperatively to promote neuroprotection. To address that, we have employed pharmacological and genetic manipulations to access neuronal cell death in primary cultured corticostriatal neurons under glutamate insult. We find that either the pharmacological blockade or genetic ablation of either mGluR5 or CB$_1$ abolishes both CB$_1$- and mGluR5-mediated neuroprotection. Moreover, these two receptors trigger the same cell signaling pathways to promote neuroprotection, which involves activation of ERK1/2 and AKT.

Methods

Materials

Neurobasal medium, N2 and B27 supplements, Gluta-MAX (50.0 mg/ml penicillin and 50 mg/ml streptomycin), Live/Dead viability assay, anti-rabbit Alexa Fluor 488 antibody, anti-mouse Alexa Fluor 546, DAPI (4′,6-Diamidino-2-Phenylindole, Dihydrochloride) and anti-PSD95 were purchased from Thermo Fisher Scientific. 3-Cyano-*N*-(1,3-diphenyl-1*H*-pyrazol-5-yl)benzamide (CDPPB), 2-methyl-6-(phenylethynyl)-pyridine (MPEP), 2-(2-Amino-3-methoxyphenyl)-4H-1-benzopyran-4-one (PD98059), 2-(4-Morpholinyl)-8-phenyl-1(4H)-benzopyran-4-one hydrochloride (LY294002), N-arachidonoy lethanolamine (anandamide), 2-Arachidonoylglycerol (2-AG) and arachidonyl-2′-chloroethylamide (ACEA) were purchased from Tocris Cookson Inc. Cyclohexyl-carbamic acid 3′-carbamoyl-biphenyl-3-yl ester (URB 597), 4-[Bis(1,3-benzodioxol-5-yl)-hydroxymethyl]piperidine-1-carboxylate 4-nitrophenyl ester (JZL184) and 1-(2,4-Dichlorophenyl)-5-(4-iodophenyl)-4-methyl-N-1-piperidinyl-1H-pyrazole-3-carboxamide (AM251) were purchased from Cayman Chemical. Horseradish peroxidase-conjugated anti-rabbit IgG secondary antibody was from BioRad. Western Blotting ECL Prime detection reagents were from GE Healthcare and Immobilon Western Chemiluminescent HRP Substrate was from Millipore. Anti-phospho AKT and anti-AKT rabbit monospecific clonal antibodies were from DB Biotech. Anti-phospho ERK1/2 (thr202/Tyr204) and anti-ERK1/2 rabbit antibodies were from Cell Signaling (USA). Anti-CB$_1$ (1–77) rabbit pAB antibody was from Calbiochem. Anti-syantaxin 1A was from Santa Cruz. All other biochemical reagents were purchased from Sigma−Aldrich.

Mouse model

C57/BL6 mice (25–30 g) were purchased from the animal facility (CEBIO) located at the Universidade Federal de Minas Gerais (UFMG). mGluR5$^{-/-}$ mice B6;129-Grm5^{tm1Rod}/J (*mGluR5$^{-/-}$*) [34] were purchased from Jackson Laboratory (Bar Harbor, ME) and PI3K$\gamma^{-/-}$ mice were kindly provided by Dr. M. M. Teixeira [51]. Mice

Batista *et al. Molecular Brain* (2016) 9:80

Page 3 of 17

were housed in an animal care facility at 23 °C on a 12 h light/12 h dark cycle with food and water provided ad libitum. Animal care was in accordance with the Universidade Federal de Minas Gerais Ethics Committee on Animal Experimentation (CETEA) and all Animal procedures were approved by CETEA/UFMG, protocol number 3/2011.

Neuronal primary culture preparation

Neuronal cultures were prepared from the striatal and cortical regions of E15 WT, mGluR5$^{-/-}$ or PI3Kγ$^{-/-}$ embryo brains. After dissection, corticostriatal tissue was submitted to trypsin digestion followed by cell dissociation using a fire-polished Pasteur pipette. Cells were plated on poly-L-ornithine coated dishes in Neurobasal medium supplemented with N2 and B27 supplements, 2 mM GlutaMAX, 50 μg/ml penicillin and 50 μg/ml streptomycin. Cells were incubated at 37 °C and 5 % CO_2 in a humidified incubator and cultured for 10 to 12 days in vitro (DIV) with medium replenishment every 4 days.

siRNA electroporation

Neurons were submitted to electroporation during preparation of primary cultures using mouse neuron Nucleofector kit (Lonza), according to manufacture instructions. Before being plated on coated dishes, a total of 2×10^6 corticostriatal neurons were incubated with the electroporation reagent and 30 pmol of either NC- or CB$_1$-siRNA (Santa Cruz). Electroporation was performed using an AMAXA nucleofector II Device apparatus and program 0–005. Neurons were then transferred to poly-L-ornithine coated dishes in supplemented Neurobasal medium. Media was replaced 4 h later and, following that, cells were incubated in the same conditions as not electroporated neurons.

Neuronal stimulation

To determine the appropriate drug concentration to be used, concentration-response experiments were performed for each drug used (data not shown), unless concentration-response curves have already being performed in previous publications from our group [10, 63]. Neuronal primary cultures obtained from WT, mGluR5 $^{-/-}$ or PI3Kγ$^{-/-}$ embryos were incubated with either vehicle (Hank's balanced salt solution: HBSS) or 50 μM glutamate, in the presence or absence of 100 nM CDPPB, 1 nM URB597, 10 nM JZL184, 10 nM anandamide, 10 nM 2-AG, 1 nM ACEA for 4 h at 37 °C, as indicated in the *Figure Legend*. When 1 μM MPEP, 10 nM AM251, 10 μM PD98059 or 1 μM LY294002 was used, it was added 5 min prior to and kept during the rest of the incubation. Following this incubation, neuronal cultures were used for cell death assays, glutamate

release experiments, [Ca^{2+}]i measurements, ERK1/2 and AKT activation assays or immunofluorescence labeling experiments.

Cell death assay

Neurons were stimulated with drugs, as indicated in the *Figure Legend*, and cell death was determined by Live/Dead viability assay, as described previously [11]. Briefly, neurons were stained with 2 μM calcein acetoxymethyl ester (AM) and 2 μM ethidium homodimer-1 for 15 min and the fractions of live (calcein AM positive) and dead (ethidium homodimer-1 positive) cells were determined. Neurons were visualized by fluorescence microscopy FLoid® Cell Imaging Station (Thermo Fisher Scientific) and scored by a blinded observer. A minimum of 150 cells were analyzed per well in triplicate using ImageJ software. Dead cells were expressed as a percentage of the total number of cells.

Glutamate release experiment

Glutamate released by primary cultured neurons was measured indirectly by the fluorescence increase due to the production of NADPH in the presence of glutamate dehydrogenase type II and NADP$^+$ [42]. Neuronal cultures seeded on 96-well plates were incubated with CaCl$_2$ (1 mM) and NADP$^+$ in HBSS and analyzed in a spectrofluorometer (Synergy 2, BioTek® Instruments, Inc.). Five min later, glutamate dehydrogenase (50 units per well) was added and reading was restarted until the fluorescence reached balance (approximately 5 min). After that, neuronal cultures were stimulated for 5 min with drugs as described in the *Figure Legend*. Calibration curves were done in parallel by adding known amounts of glutamate (5 nM/μl) to the reaction medium. The experimental data were expressed as percentage, taking glutamate released by neurons stimulated with 50 μM glutamate as 100 %. The experiments were performed at 37 °C, in duplicate well for each condition, with excitation wavelength of 360 nm and emission of 450 nm.

Measurement of intracellular Ca^{2+} concentration

Neuronal cultures seeded on 96-well plates were loaded with 0.2 μM Fura-2 AM for 20 min at 37 °C and stimulated with drugs, as described in the *Figure Legend*. Neurons were washed with HBSS and illuminated with alternating 340- and 380-nm light, with the 510-nm emission detected using a spectrofluorometer. At the end of each experiment sodium dodecyl sulfate (SDS) 10 % (0.1 % final) was added to obtain R_{max} followed by 3 M Tris + 400 mM EGTA (pH 8.6) for R_{min}, as described by [16]. The increase in [Ca^{2+}]$_i$ promoted by 50 μM glutamate was taken as 100 %. All experiments were performed in triplicate wells for each condition.

Batista et al. Molecular Brain (2016) 9:80

Page 4 of 17

Immunoblotting

Following drug stimulation, neurons were lysed in RIPA buffer (0.15 M NaCl, 0.05 M Tris-HCl, pH 7.2, 0.05 M EDTA, 1 % nonidet P40, 1 % Triton X-100, 0.5 % sodium deoxycholate, 0.1 % SDS) containing protease inhibitors (1 mM AEBSF and 10 μg/ml of both leupeptin and aprotinin). 100 μg of total cellular protein for each sample was subjected to SDS-PAGE, followed by electroblotting onto nitrocellulose membranes. Membranes were blocked with 5 % BSA in wash buffer (150 mM NaCl, 10 mM Tris–HCl, pH 7.4, and 0.05 % Tween 20) for 1 h and then incubated with either rabbit anti-phospho AKT (S473) (1:1000) or rabbit anti-phospho ERK1/2 (Thr202/Thr204) (1:1000) antibodies in wash buffer containing 3 % BSA for 2 h at room temperature. Membranes were rinsed three times with wash buffer and then incubated with secondary peroxidase-conjugated anti-rabbit IgG antibody diluted 1:5000 in wash buffer containing 3 % skim milk for 1 h. Membranes were rinsed three times with wash buffer, incubated with ECL prime western blotting detection reagents and scanned and analysed by ImageQuant LAS 4000 (GE Healthcare). Antibodies were then stripped and membranes were incubated with either rabbit anti-AKT (1:1000) or rabbit anti-ERK1/2 (1:1000) antibodies for 2 h and probed with secondary antibody anti-rabbit IgG 1:5000 to determine total AKT and ERK1/2 expression. Non-saturated, immunoreactive AKT and ERK1/2 bands were quantified by scanning densitometry. Immuno-band intensity was calculated using ImageJ software and the number of pixels of AKT and ERK1/2 phospho-bands was divided by the number of pixels of total AKT and ERK1/2 to normalize phosphorylation levels of kinases to total kinase expression. In the case of CB_1 protein expression assessments, membranes were blocked with 5 % skim milk and 5 % BSA in wash buffer (150 mM NaCl, 10 mM Tris-HCl, pH 7.4, and 0.1 % Tween 20) for 24 h and then incubated with either rabbit anti-CB_1 (1:1000) or rabbit anti-actin (1:1000) antibodies in wash buffer containing 3 % skim milk overnight at 4 °C. Membranes were rinsed three times with wash buffer and then incubated with secondary peroxidase-conjugated anti-rabbit IgG antibody diluted 1:5000 in wash buffer containing 3 % skim milk for 1 h. Membranes were rinsed three times with wash buffer, incubated with ECL western blotting detection reagents and scanned and analysed by ImageQuant LAS 4000.

Immunofluorescence and imaging

Corticostriatal neurons were stimulated, as describe in the *Figure Legend*, washed twice in PBS and fixed with 4 % formaldehyde in PBS for 20 min. After fixation, cells were washed with PBS and preincubated with a permeabilization solution (PBS, 0.2 % Triton, and 1 % bovine serum albumin) for 20 min. Following that, mouse anti-syntaxin 1A (1:500) or rabbit anti-PSD95 (1:500) antibodies were added to cells and incubated in permeabilization solution for 16 h at 4 ° C. Cells were washed and incubated with goat anti-mouse and anti-rabbit antibodies conjugated to Alexa Fluor 546 1:500 and Alexa Fluor 488 1:500, respectively, for 60 min in permeabilization solution. Following that, cells were washed and stained with DAPI 1:1000 for 10 min. Fluorescence microscopy was performed using a Zeiss LSM 880 confocal system equipped with a 40x/1.30 oil DIC M27 objective. Image acquisition was done by a blind observer using the Zen 2 software. Settings for wavelength detection of immunolabeled proteins were adjusted as follows: DAPI was imaged by detection between 410 and 496 nm, Alexa Fluor 488-labeled anti-PSD95 antibody was detected between 499 and 552 nm, and Alexa Fluor 546-labeled anti-syntaxin 1A antibody was detected between 552 and 679 nm. Sequential excitation of fluorophores was performed using 405, 488, 532 nm lasers for DAPI, Alexa Fluor 488 and Alexa Fluor 546, respectively. Fluorescence intensity of pixel grey levels was obtained using ImageJ software and total intensity was normalized by the total number of cells (DAPI-labeled nucleus).
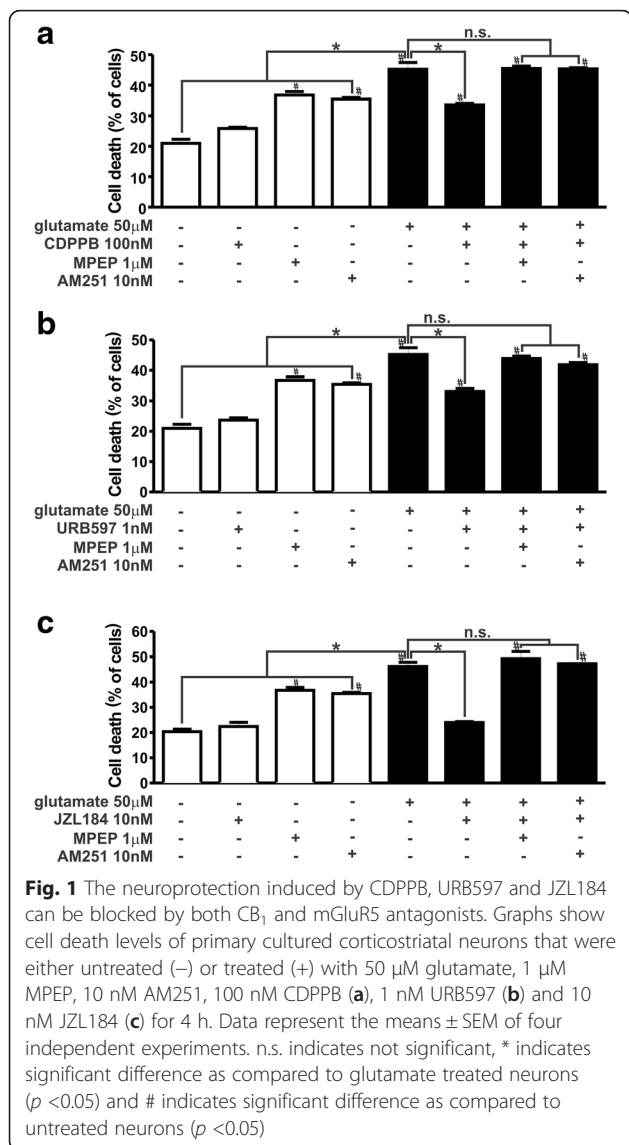
Data analysis

Means ± SEM are shown for the number of independent experiments indicated in *Figure Legends*. GraphPad Prism™ software was used to analyze data for statistical significance. Statistical significance (p <0.05) was determined by analysis of variance (ANOVA) testing followed by Bonferroni post-hoc Multiple Comparison Testing.

Results

The neuroprotection induced by CDPPB, URB597 and JZL184 can be blocked by both CB_1 and mGluR5 antagonists

We have previously demonstrated that CDPPB, an mGluR5 PAM, promotes survival of primary cultured striatal neurons and rescues the neuronal cell loss observed in a mouse model of HD [10, 11]. In order to investigate whether CB_1 could be involved in mGluR5-mediated neuroprotection, we prepared primary neuronal cultures from the cortex and striatum, which contain mostly GABAergic and glutamatergic neurons [11, 40]. Incubation of these cultures with 50 μM glutamate for 4 h promoted the death of 45–50 % of the cells (Fig. 1). Next, we performed concentration-response experiments to determine the concentrations of MPEP and AM251 that were effective to block mGluR5 and CB_1, respectively, without leading to high levels of neuronal death. We found that 1 μM MPEP and 10 nM AM251 were the lowest concentrations of

Batista et al. Molecular Brain (2016) 9:80

Page 5 of 17

Fig. 1 The neuroprotection induced by CDPPB, URB597 and JZL184 can be blocked by both CB_1 and mGluR5 antagonists. Graphs show cell death levels of primary cultured corticostriatal neurons that were either untreated (–) or treated (+) with 50 μM glutamate, 1 μM MPEP, 10 nM AM251, 100 nM CDPPB (**a**), 1 nM URB597 (**b**) and 10 nM JZL184 (**c**) for 4 h. Data represent the means ± SEM of four independent experiments. n.s. indicates not significant, * indicates significant difference as compared to glutamate treated neurons (p <0.05) and # indicates significant difference as compared to untreated neurons (p <0.05)

antagonists that were effective to block the receptors (data not shown). Although the levels of neuronal cell death triggered by both antagonists were higher than basal levels, they were not as high as glutamate-induced neuronal cell death (Fig. 1). Thus, 1 μM MPEP and 10 nM AM251 were the concentrations used in this study.
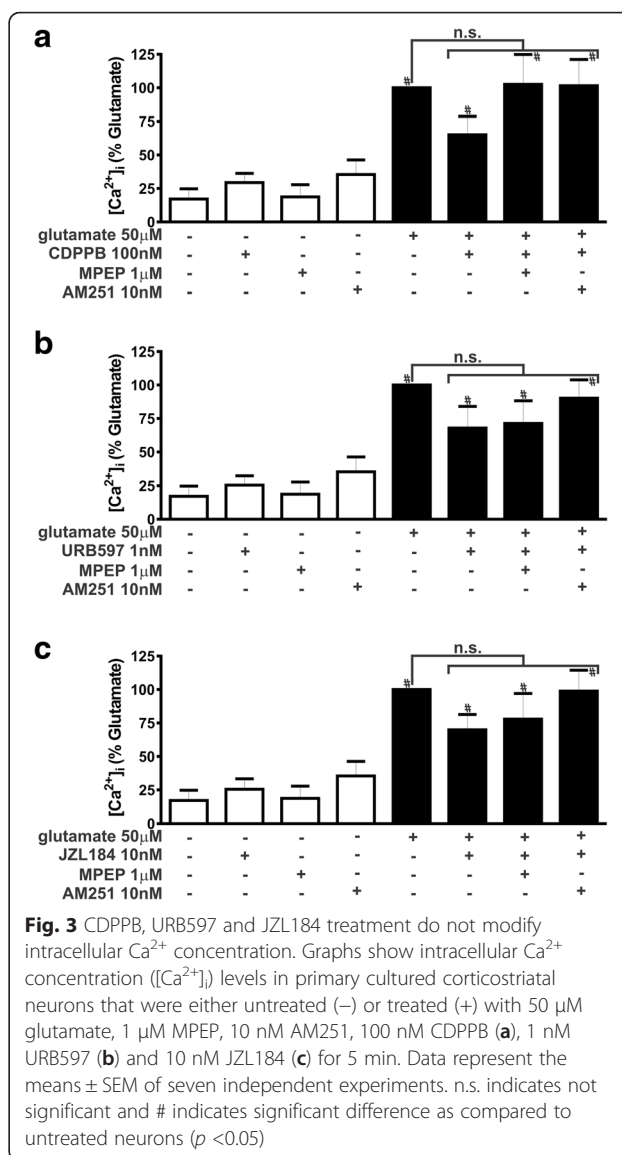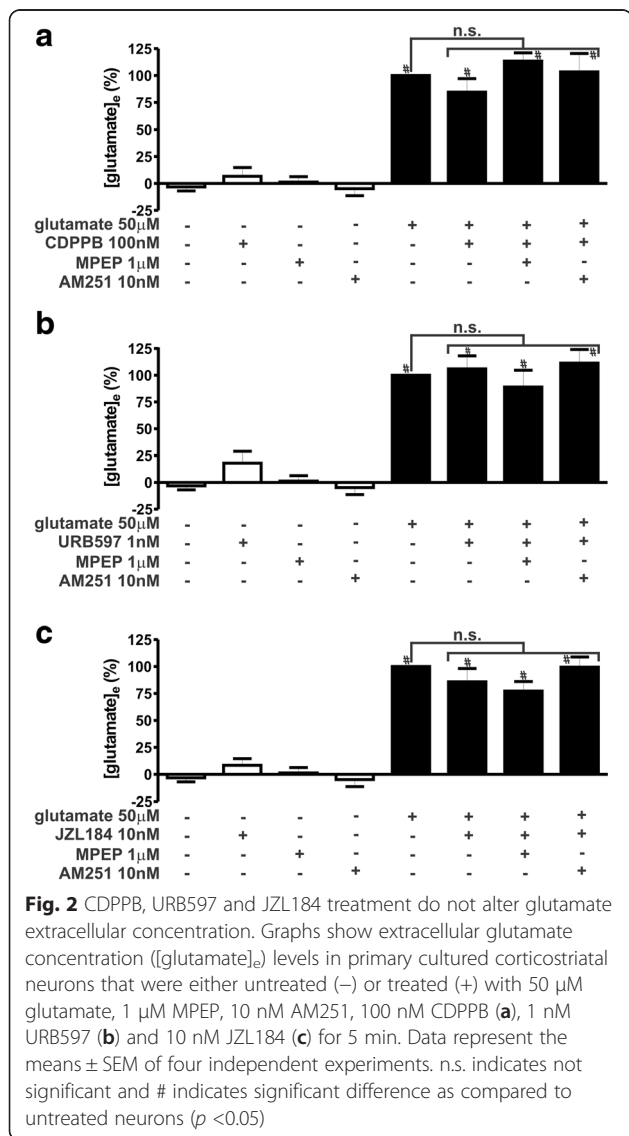
In agreement with previously published data from our group, 100 nM CDPPB prevented glutamate-induced neuronal cell death and the mGluR5 antagonist MPEP (1 μM) abrogated CDPPB-induced neuroprotection ($F_{7,32} = 72.66$, p <0.0001; Fig. 1a). To check whether CB_1 was involved in CDPPB-mediated neuroprotection, neurons were pre-treated with the CB_1 antagonist, AM251. Interestingly, 10 nM AM251 efficiently abolished CDPPB-induced neuroprotection (Fig. 1a), indicating that CB_1 was involved in mGluR5-mediated neuroprotection.

There are many pharmacological tools to manipulate the cannabinoid system. Anandamide and 2-AG are direct agonists of cannabinoid receptors. However, these compounds are very rapidly degraded by the enzymes fatty acid amide hydrolase (FAAH) and monoacylglycerol lipase (MGL), respectively [9, 20, 60]. On the other hand, the degrading enzymes FAAH and MGL can be inhibited by URB597 and JZL184, respectively, increasing the levels of endocannabinoids [27, 33]. To test whether increased levels of anandamide and 2-AG could rescue cell death promoted by 50 μM glutamate, corticostriatal neurons were treated with either 1 nM URB597 or 10 nM JZL184. Both URB597 ($F_{7,32} = 58.67$, p <0.0001; Fig. 1b) and JZL184 ($F_{7,24} = 60.18$, p <0.0001; Fig. 1c) were efficient to promote neuroprotection under these conditions. Induction of neuroprotection was dependent on CB_1, as AM251 blocked both URB597- (Fig. 1b) and JZL184-induced (Fig. 1c) neuronal survival. However, MPEP was also capable of abrogating URB597- (Fig. 1b) and JZL184-induced (Fig. 1c) neuroprotection. mGluR5 was previously shown to be important for endocannabinoid synthesis and its blockade can diminish endogenous levels of cannabinoids [23, 25]. Thus, we hypothesized that when mGluR5 was blocked, inhibition of endocannabinoid degradation would not increase cannabinoids to levels high enough to promote neuroprotection. In this case, CB_1 direct agonist would be able to promote neuroprotection even if mGluR5 was blocked. To test this hypothesis, we used cannabinoid receptors direct agonists, including anandamide and 2-AG, as well as ACEA, a CB_1 specific agonist, to rescue glutamate-induced neuronal cell death. The three tested cannabinoid receptor direct agonists were capable of rescuing glutamate-induced neuronal cell death and AM251 was efficient to block this effect ($F_{13,70} = 76.98$, p <0.0001; Additional file 1: Figure S1). However, mGluR5 blockade by MPEP only partially abolished anandamide-, 2-AG- and ACEA-induced neuronal survival (Additional file 1: Figure S1). Thus, mGluR5 activity was not as important when CB_1 direct agonists were used, as there was no need for endocannabinoid synthesis.

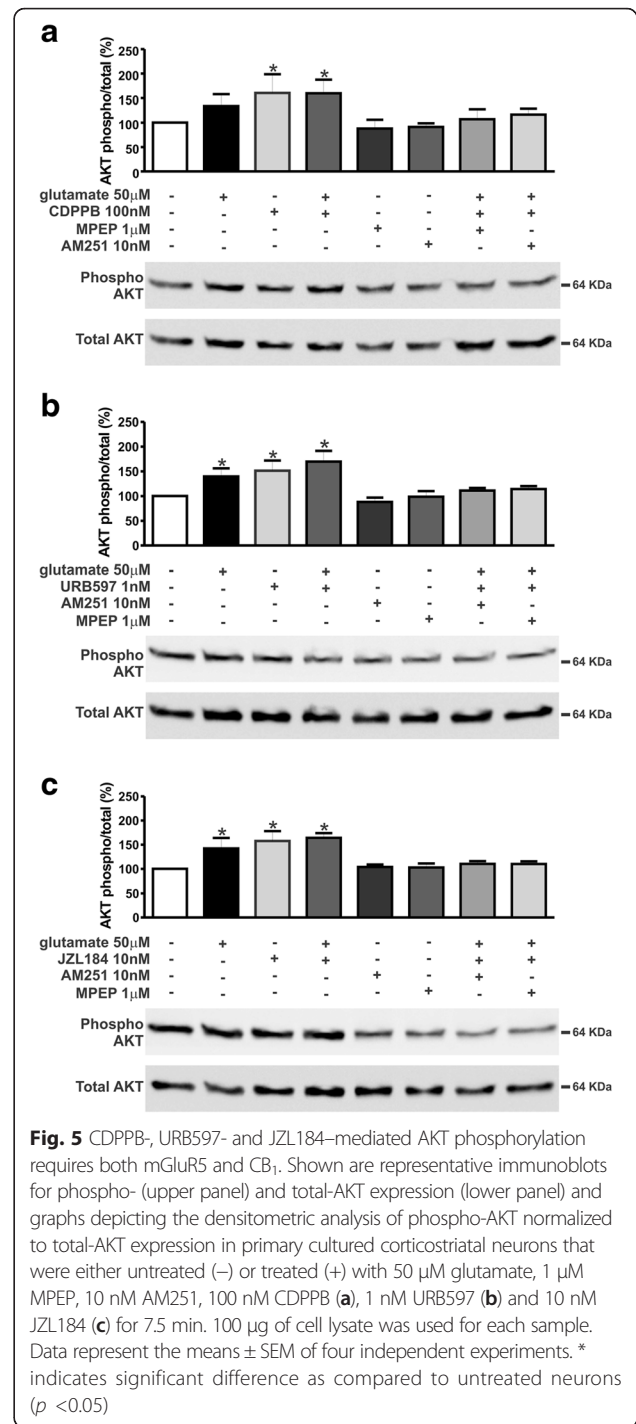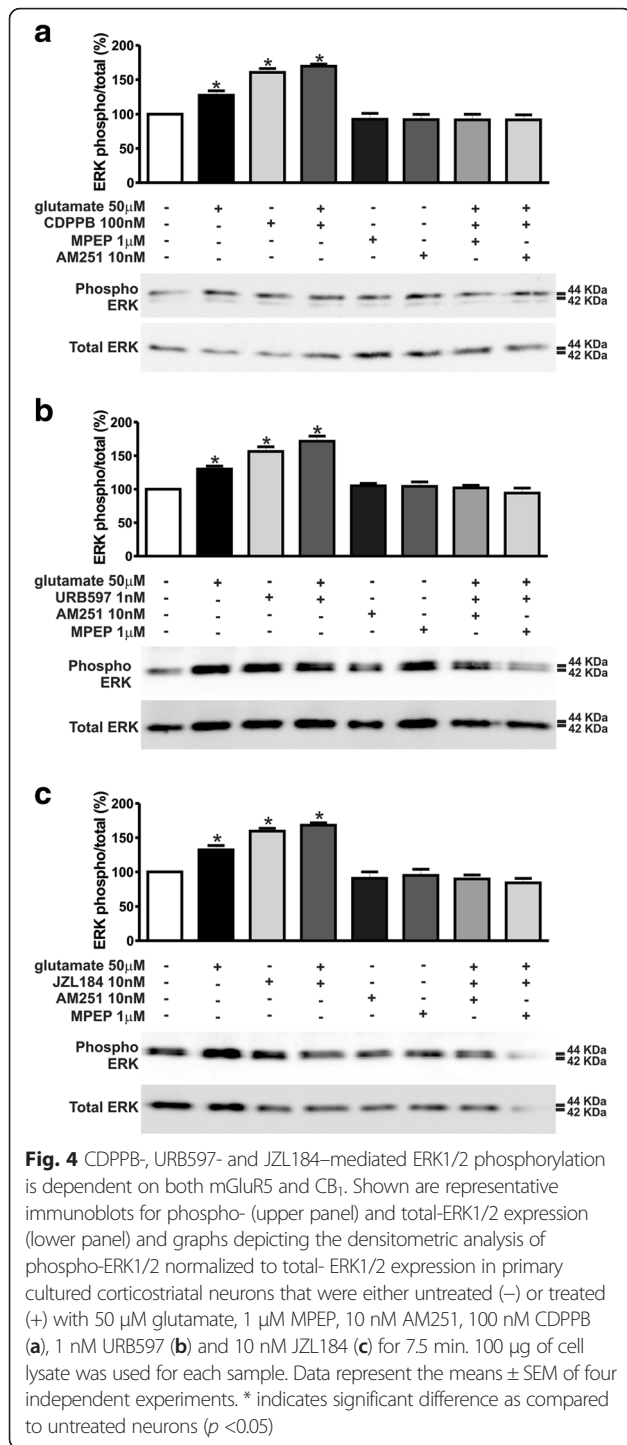## CDPPB, URB597 and JZL184 treatment activate ERK1/2 and AKT

Our next step was to determine whether mGluR5 and CB_1 employ similar mechanisms to trigger neuroprotection. Decreased release of glutamate by glutamatergic pre-synaptic sites was proposed to be one of the neuroprotective mechanisms elicited by CB_1 activation [36, 52]. Thus, we investigated whether the neuroprotective drugs could diminish glutamate release. In the absence of glutamate insult, none of the tested drugs, CDPPB, URB597, JZL184, MPEP and AM251, modified

Batista *et al. Molecular Brain* (2016) 9:80

Page 6 of 17

glutamate release, as compared to basal levels (Fig. 2). Moreover, in the presence of glutamate, CDPPB ($F_{7,28} = 30.84$, $p < 0.0001$; Fig. 2a), URB597 ($F_{7,28} = 26.50$, $p < 0.0001$; Fig. 2b) and JZL184 ($F_{7,27} = 39.25$, $p < 0.0001$; Fig. 2c) were also not efficient to modify extracellular glutamate levels. It has been shown that endocannabinoids can decrease glutamate release. However, as the cell death insult used in this study was glutamate itself, it was likely that decreasing glutamate release would not play a major role in the neuroprotective mechanism. We also measured intracellular Ca^{2+} levels in these neuronal cultures, as one possible cell survival mechanism would be to decrease the intracellular levels of this ion. Similarly, none of the tested drugs increased intracellular Ca^{2+} above basal levels in the absence of glutamate (Fig. 3). Incubation of neuronal cultures with glutamate induced high levels of intracellular Ca^{2+} (Fig. 3), which could contribute to neuronal excitotoxicity.

Fig. 2 CDPPB, URB597 and JZL184 treatment do not alter glutamate extracellular concentration. Graphs show extracellular glutamate concentration ([glutamate]$_e$) levels in primary cultured corticostriatal neurons that were either untreated (−) or treated (+) with 50 μM glutamate, 1 μM MPEP, 10 nM AM251, 100 nM CDPPB (**a**), 1 nM URB597 (**b**) and 10 nM JZL184 (**c**) for 5 min. Data represent the means ± SEM of four independent experiments. n.s. indicates not significant and # indicates significant difference as compared to untreated neurons ($p < 0.05$)

Fig. 3 CDPPB, URB597 and JZL184 treatment do not modify intracellular Ca^{2+} concentration. Graphs show intracellular Ca^{2+} concentration ([Ca^{2+}]$_i$) levels in primary cultured corticostriatal neurons that were either untreated (−) or treated (+) with 50 μM glutamate, 1 μM MPEP, 10 nM AM251, 100 nM CDPPB (**a**), 1 nM URB597 (**b**) and 10 nM JZL184 (**c**) for 5 min. Data represent the means ± SEM of seven independent experiments. n.s. indicates not significant and # indicates significant difference as compared to untreated neurons ($p < 0.05$)

However, CDPPB ($F_{7,54} = 8.259$, $p < 0.0001$; Fig. 3a), URB597 ($F_{7,54} = 8.300$, $p < 0.0001$; Fig. 3b) and JZL184 ($F_{7,54} = 9.179$, $p < 0.0001$; Fig. 3c) did not modify glutamate-induced increased levels of intracellular Ca^{2+}. Therefore, the cell survival mechanism elicited by CDPPB, URB597 and JZL184 in neurons treated with glutamate did not appear to involve either reduced glutamate release or decreased intracellular Ca^{2+} levels.

As both mGluR5 and CB_1 can activate similar cell survival pathways, we investigated whether activation of ERK1/2 and AKT could be involved in the mGluR5/CB_1 neuroprotective mechanism. Stimulation of corticostriatal neuronal cultures with CDPPB was efficient to promote phosphorylation and thus activation of both ERK1/2 ($F_{7,24} = 25.43$, $p < 0.0001$; Fig. 4a) and AKT ($F_{7,24} = 7.083$, $p = 0.0001$; Fig. 5a) above basal levels, either in the absence or presence of glutamate. Both MPEP and

Batista *et al. Molecular Brain* (2016) 9:80

Page 7 of 17

Fig. 4 CDPPB-, URB597- and JZL184–mediated ERK1/2 phosphorylation is dependent on both mGluR5 and CB$_1$. Shown are representative immunoblots for phospho- (upper panel) and total-ERK1/2 expression (lower panel) and graphs depicting the densitometric analysis of phospho-ERK1/2 normalized to total- ERK1/2 expression in primary cultured corticostriatal neurons that were either untreated (−) or treated (+) with 50 μM glutamate, 1 μM MPEP, 10 nM AM251, 100 nM CDPPB (**a**), 1 nM URB597 (**b**) and 10 nM JZL184 (**c**) for 7.5 min. 100 μg of cell lysate was used for each sample. Data represent the means ± SEM of four independent experiments. * indicates significant difference as compared to untreated neurons (*p* <0.05)

Fig. 5 CDPPB-, URB597- and JZL184–mediated AKT phosphorylation requires both mGluR5 and CB$_1$. Shown are representative immunoblots for phospho- (upper panel) and total-AKT expression (lower panel) and graphs depicting the densitometric analysis of phospho-AKT normalized to total-AKT expression in primary cultured corticostriatal neurons that were either untreated (−) or treated (+) with 50 μM glutamate, 1 μM MPEP, 10 nM AM251, 100 nM CDPPB (**a**), 1 nM URB597 (**b**) and 10 nM JZL184 (**c**) for 7.5 min. 100 μg of cell lysate was used for each sample. Data represent the means ± SEM of four independent experiments. * indicates significant difference as compared to untreated neurons (*p* <0.05)

AM251 were efficient to block ERK1/2 (Fig. 4a) and AKT (Fig. 5a) activation, suggesting that stimulation of mGluR5 by CDPPB requires CB$_1$ activation. Moreover, URB597 and JZL184 were also efficient to activate ERK1/2 ($F_{7,24}$ = 27.03, *p* <0.0001; Fig. 4b and $F_{7,24}$ = 29.12, *p* <0.0001; c) and AKT ($F_{7,24}$ = 18.37, *p* <0.0001; Fig. 5b and $F_{7,24}$ = 19.68, *p* <0.0001; 5C) above basal levels, either in the absence or presence of glutamate. As in the case of CDPPB, both MPEP and AM251 eliminated ERK1/2 (Fig. 4b and c) and AKT (Fig. 5b and c) activation by URB597 and JZL184. Together, these data suggested that both mGluR5 and CB$_1$ were necessary for the activation of important neuronal survival cell signaling pathways.

Batista *et al. Molecular Brain* (2016) 9:80

Page 8 of 17

CDPPB, URB597 and JZL184 treatment are unable to activate ERK1/2 and AKT and promote neuroprotection of either mGluR5$^{-/-}$ or CB1 knockdown neurons

To determine whether the results obtained following pharmacological blockade of the receptors could be reproduced by genetic knockout, we employed primary cultured corticostriatal neurons obtained from mGluR5$^{-/-}$ embryos to test the neuroprotective drugs. Interestingly, basal neuronal cell death was already higher in the case of mGluR5$^{-/-}$ neurons, as compared to that of mGluR5$^{+/+}$ neurons ($F_{7,72}$ = 194.00, p <0.0001; Fig. 6a). Moreover, treatment with CDPPB, URB597 and JZL184, in the absence of glutamate, elicited higher levels of neuronal cell death in mGluR5$^{-/-}$ neurons than in mGluR5$^{+/+}$ neurons (Fig. 6a). However, glutamate insult promoted higher levels of neuronal cell death in mGluR5$^{+/+}$ neurons than in mGluR5$^{-/-}$ neurons (Fig. 6a). These data further highlighted the vital role of mGluR5 in cell death mechanisms. Importantly, although CDPPB, URB597 and JZL184 promoted neuroprotection against glutamate insult in mGluR5$^{+/+}$ neurons, these drugs failed to promote survival of mGluR5$^{-/-}$ neurons (Fig. 6a). In addition, CDPPB, URB597 and JZL184 were only able to activate ERK1/2 and AKT in mGluR5$^{+/+}$ neurons ($F_{7,24}$ = 32.95, p <0.0001; Fig. 6b and $F_{7,24}$ = 14.58, p <0.0001; d), but not in mGluR5$^{-/-}$ neurons ($F_{7,32}$ = 2.674, p = 0,0262; Fig. 6c and $F_{7,24}$ = 4.475, p = 0.0026; e).

To determine whether a decrease in CB$_1$ protein expression could compromise neuroprotection via mGluR5 and CB$_1$, we electroporated CB$_1$ small interfering RNA (siRNA) into corticostriatal neurons to knockdown CB$_1$ expression. A negative control (NC) siRNA, which did not target murine mRNAs, was also used. CB$_1$-siRNA efficiently knockdown CB$_1$ protein expression by 55 %, as compared to NC-siRNA (Additional file 2: Figure S2). Basal neuronal cell death levels were not different when comparing neurons electroporated with either CB$_1$-siRNA or NC-siRNA ($F_{7,48}$ = 157.4, p <0.0001; Fig. 7a). However, stimulation of neurons with CDPPB, URB597 and JZL184, in the absence of glutamate, triggered higher cell death levels of CB$_1$ knockdown neurons than of control neurons (Fig. 7a). These data indicated that compromised expression of CB$_1$ could render neurons more sensitive to the toxic effects of drugs, further supporting the premise that CB$_1$ plays a key role in cell survival mechanisms. Glutamate insult increased cell death levels to the same extent when comparing NC-siRNA or CB$_1$-siRNA electroporated neurons (Fig. 7a). As in the case of mGluR5$^{-/-}$, CDPPB, URB597 and JZL184 were not able to protect CB$_1$ knockdown neurons against glutamate insult, although these drugs were efficient to protect control neurons exposed to glutamate (Fig. 7a). Moreover, CDPPB, URB597 and JZL184 were only capable of activating ERK1/2 and AKT in control neurons ($F_{7,24}$ = 7.929, p <0.0001; Fig. 7b and $F_{7,24}$ = 5.252, p = 0,0010; d), but not in CB$_1$ knockdown neurons ($F_{7,24}$ = 5.231, p =

0.0010; Fig. 7c and $F_{7,24}$ = 2.649, p = 0.0352; e). These data further support the hypothesis that mGluR5 and CB$_1$ act in a cooperative manner to activate cell signaling pathways that lead to neuroprotection.

Neuroprotection induced by CDPPB, URB597 and JZL184 is dependent on both ERK1/2 and AKT

To determine whether AKT was indeed necessary for CB$_1$ and mGluR5 neuroprotection, we performed cell death experiments in corticostriatal neurons obtained from mice knockout for the phosphatidylinositol-3 kinase γ (PI3Kγ$^{-/-}$), as PI3K is a key component that is upstream from AKT activation by mGluRs and CB$_1$ [15, 50]. In the absence of glutamate, PI3Kγ$^{-/-}$ neurons incubated with CDPPB and URB597 exhibited higher levels of neuronal cell death than those of PI3Kγ$^{+/+}$ neurons ($F_{7,64}$ = 175.3, p <0.0001; Fig. 8a), possibly because PI3Kγ knockout decreased activation of cell survival pathways and made neurons more prone to toxicity. Although CDPPB, URB597 and JZL184 promoted neuroprotection of PI3Kγ$^{+/+}$ neurons under the insult of glutamate, neuroprotection triggered by these drugs was partially abrogated in PI3Kγ$^{-/-}$ neurons incubated with glutamate (Fig. 8a). Moreover, CDPPB, URB597 and JZL184 failed to activate AKT in PI3Kγ$^{-/-}$ neurons ($F_{7,16}$ = 7.03, p = 0.0006; Additional file 3: Figure S3). However, in the presence of glutamate, CDPPB, URB597 and JZL184 were still able to increase AKT phosphorylation above basal levels in PI3Kγ$^{-/-}$ neurons (Additional file 3: Figure S3). It has been shown that GPCRs can activate AKT through both PI3Kγ and PI3Kβ and that these kinases may thus have a redundant function [17]. Therefore, it was possible that other PI3K isoforms, including PI3Kβ, could also contribute to AKT activation when neurons were stimulated with the tested drugs in the presence of glutamate, which could explain why neuroprotection was not completely eliminated in PI3Kγ$^{-/-}$ neurons. To further investigate the role of AKT activation in CDPPB-, URB597- and JZL184-mediated neuroprotection, we pre-incubated neurons with 1 μM of LY294002, which inhibited all PI3K isoforms that were relevant to neuroprotective mechanisms [64]. LY294002 completely abrogated neuronal protection triggered by CDPPB, URB597 and JZL184 ($F_{8,27}$ = 91.34, p <0.0001; Fig. 8b), strongly indicating that the PI3K/AKT pathway was necessary for CB$_1$- and mGluR5-mediated neuroprotection. To determine whether ERK1/2 activation was also important for mGluR5/CB$_1$-mediated neuroprotection, we inhibited the mitogen-activated protein kinase kinase (MEK), the main kinase responsible for ERK1/2 activation. Inhibition of MEK using 10 μM PD98059 eliminated the neuroprotection prompted by CDPPB, URB597 and JZL184 ($F_{8,27}$ = 155.7, p <0.0001; Fig. 8c). Taken together, these data strongly indicated that CB$_1$ and mGluR5 mediated neuroprotection depends on both PI3K/AKT and MEK/ERK1/2 pathways.

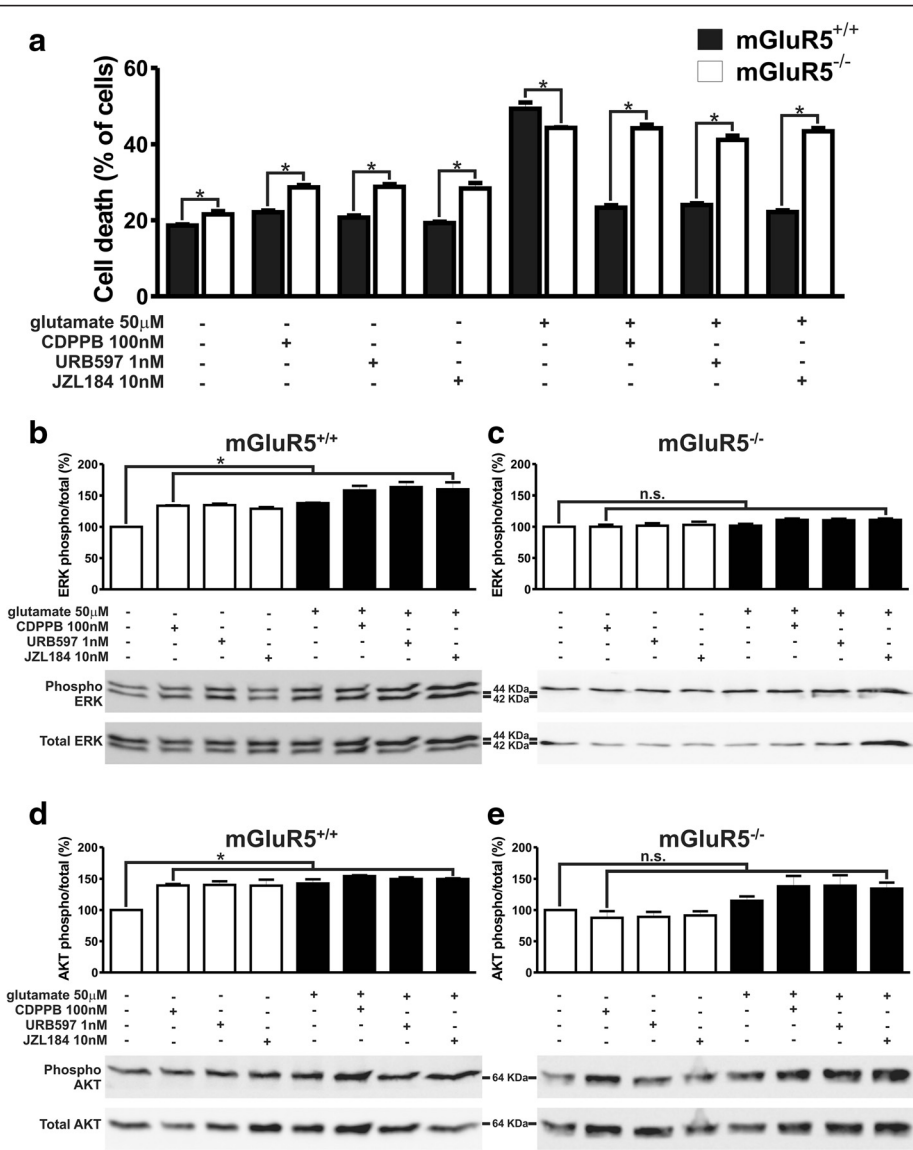Batista *et al. Molecular Brain* (2016) 9:80

Page 9 of 17

Fig. 6 CDPPB, URB597 and JZL184 treatment are unable to activate ERK1/2 and AKT and promote neuroprotection of mGluR5$^{-/-}$ neurons. **a** Graph shows cell death levels of corticostriatal neurons from either mGluR5$^{+/+}$ or mGluR5$^{-/-}$ embryos that were either untreated (−) or treated (+) with 50 μM glutamate, 100 nM CDPPB, 1 nM URB597 and 10 nM JZL184 for 4 h. Data represent the means ± SEM of four independent experiments. * indicates significant difference as compared to matched treated mGluR5$^{+/+}$ neurons (*p* <0.05). Shown are representative immunoblots for phospho- (*upper* panel) and total-ERK1/2 expression (*lower* panel) and graphs depicting the densitometric analysis of phospho-ERK1/2 normalized to total- ERK1/2 expression in primary cultured corticostriatal neurons from either mGluR5$^{+/+}$ (**b**) or mGluR5$^{-/-}$ (**c**) embryos that were either untreated (−) or treated (+) with 50 μM glutamate, 100 nM CDPPB, 1 nM URB597 and 10 nM JZL184 for 7.5 min. Also shown are representative immunoblots for phospho- (*upper* panel) and total-AKT expression (*lower* panel) and graphs depicting the densitometric analysis of phospho-AKT normalized to total-AKT expression in primary cultured corticostriatal neurons from either mGluR5$^{+/+}$ (**d**) or mGluR5$^{-/-}$ (**e**) embryos that were either untreated (−) or treated (+) with 50 μM glutamate, 100 nM CDPPB, 1 nM URB597 and 10 nM JZL184 for 7.5 min. 100 μg of cell lysate was used for each sample. Data represent the means ± SEM of four independent experiments. n.s. indicates not significant and * indicates significant difference as compared to untreated neurons (*p* <0.05)

CDPPB protects the postsynaptic site and JZL184 mainly protects presynaptic terminals

The loss of synaptic terminals can be regarded as the most important feature of neurodegeneration as synaptic loss better correlates with disease progression than neuronal cell loss itself [19, 59]. mGluR5 is mostly expressed at the post-synaptic site and CB$_1$ is mainly pre-synaptic [29, 53]. Thus, we decided to investigate whether mGluR5 and CB$_1$ activation could prevent the loss of pre- and/or post-synaptic terminals following glutamate insult. To test this, we treated neurons with the previously tested drugs and performed immunofluorescence
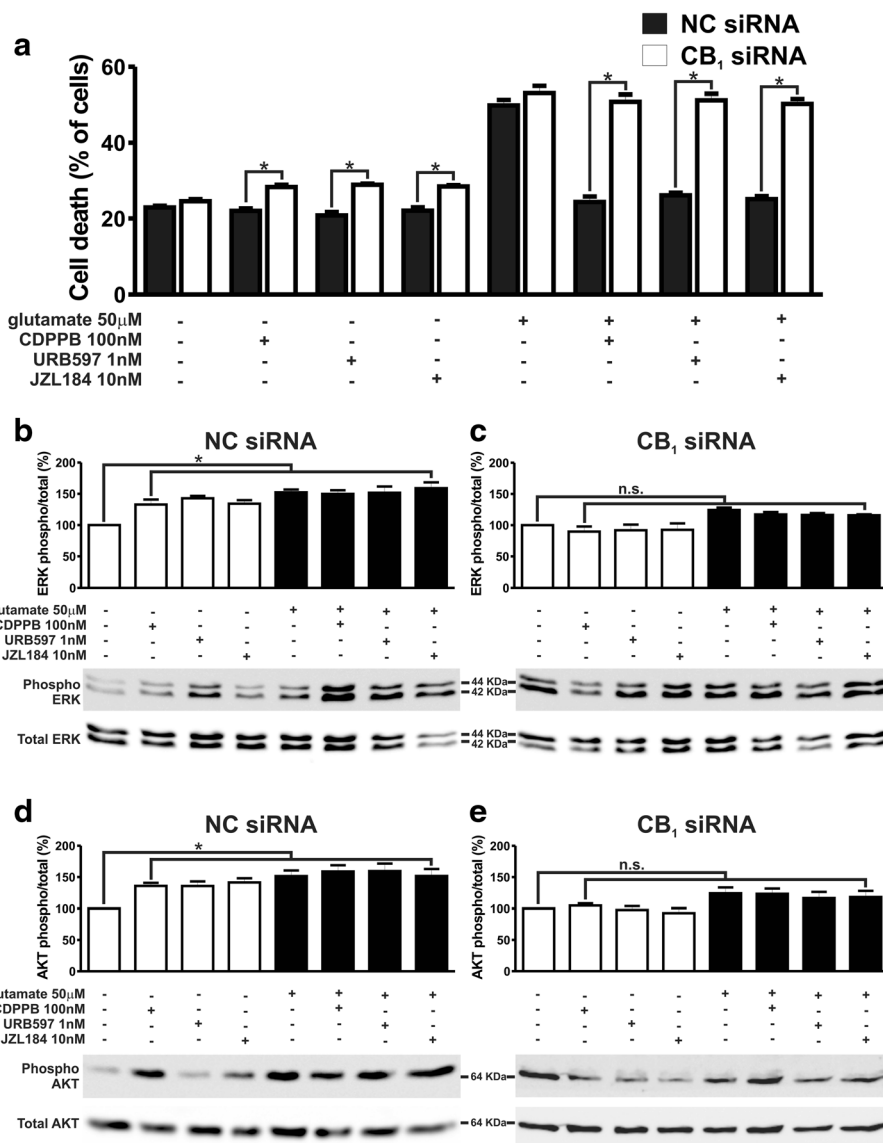
Batista *et al. Molecular Brain* (2016) 9:80

Page 10 of 17

Fig. 7 CDPPB, URB597 and JZL184 treatments fail to activate ERK1/2 and AKT and promote neuroprotection of CB₁ knockdown neurons. **a** Graph shows cell death levels of corticostriatal neurons that were electroporated with either NC- or CB₁-siRNA and that were either untreated (−) or treated (+) with 50 μM glutamate, 100 nM CDPPB, 1 nM URB597 and 10 nM JZL184 for 4 h. Data represent the means ± SEM of four independent experiments. * indicates significant difference as compared to matched treated NC-siRNA electroporated neurons (p <0.05). Shown are representative immunoblots for phospho- (*upper* panel) and total-ERK1/2 expression (*lower* panel) and graphs depicting the densitometric analysis of phospho-ERK1/2 normalized to total-ERK1/2 expression in primary cultured corticostriatal neurons that were electroporated with either NC- (**b**) or CB₁-siRNA (**c**) and that were either untreated (−) or treated (+) with 50 μM glutamate, 100 nM CDPPB, 1 nM URB597 and 10 nM JZL184 for 7.5 min. Also shown are representative immunoblots for phospho- (upper panel) and total-AKT expression (lower panel) and graphs depicting the densitometric analysis of phospho-AKT normalized to total-AKT expression in primary cultured corticostriatal neurons that were electroporated with either NC- (**d**) or CB₁-siRNA (**e**) and that were either untreated (−) or treated (+) with 50 μM glutamate, 100 nM CDPPB, 1 nM URB597 and 10 nM JZL184 for 7.5 min. 100 μg of cell lysate was used for each sample. Data represent the means ± SEM of four independent experiments. n.s. indicates not significant and * indicates significant difference as compared to untreated neurons (p <0.05)

experiments to label the postsynaptic density protein, PSD95, and the presynaptic marker, syntaxin 1A, and then quantified the levels of post- and pre-synaptic loss. 50 μM glutamate promoted a significant decrease in PSD95 and syntaxin 1A labeling (Fig. 9b, $F_{7,203} = 7.765$, p <0.0001; e and $F_{7,198} = 11.01$, p <0.0001; f), as compared to untreated

neurons (Fig. 9a, e and f), indicating that this neurotransmitter could trigger the loss of both post- and pre-synaptic terminals. When neurons were incubated with glutamate in the presence of CDPPB, the loss of PSD95 labeling was rescued (Fig. 9c and e). Although CDPPB augmented syntaxin levels, this increase was

Batista *et al. Molecular Brain* (2016) 9:80
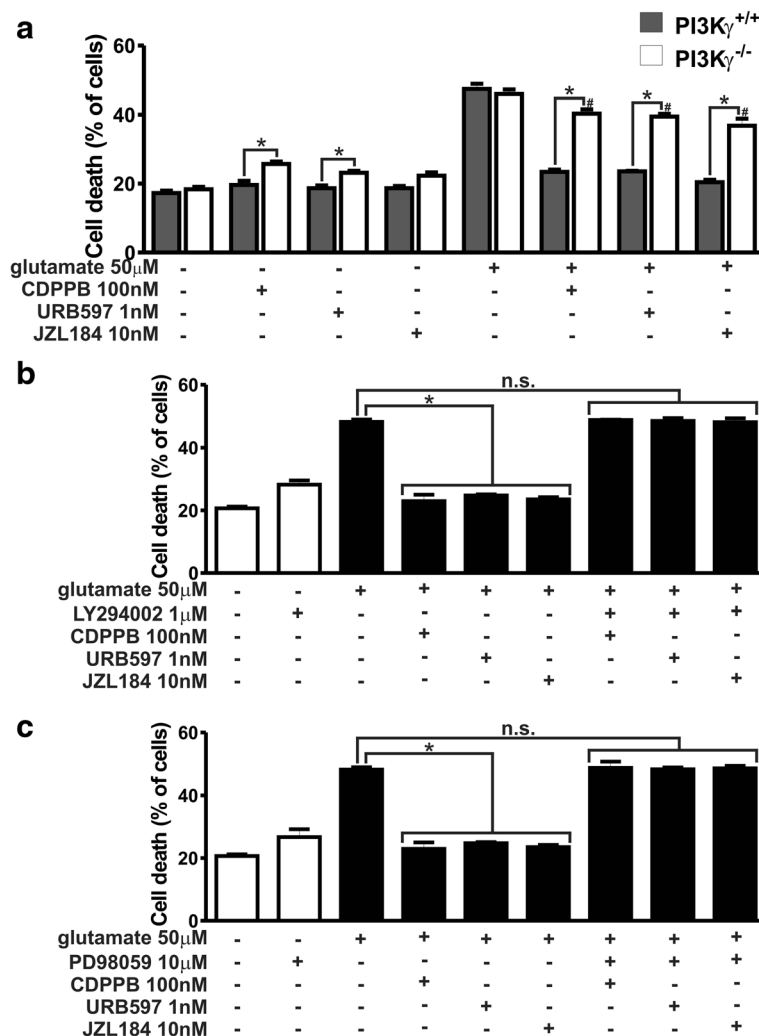
Page 11 of 17

Fig. 8 Neuroprotection induced by CDPPB, URB597 and JZL184 is dependent on both ERK1/2 and AKT. **a** Graph shows cell death levels of corticostriatal neurons from either PI3Kγ$^{+/+}$ or PI3Kγ$^{-/-}$ embryos that were either untreated (−) or treated (+) with 50 μM glutamate, 100 nM CDPPB, 1 nM URB597 and 10 nM JZL184 for 4 h. Data represent the means ± SEM of four independent experiments. * indicates significant difference as compared to matched treated PI3Kγ$^{+/+}$ neurons and # indicates significant difference as compared to glutamate-treated PI3Kγ$^{-/-}$ neurons ($p < 0.05$). Graphs show cell death levels of primary cultured corticostriatal neurons that were either untreated (−) or treated (+) with 50 μM glutamate, 100 nM CDPPB, 1 nM URB597, 10 nM JZL184, 1 μM LY294002 (**b**) and 10 μM PD98059 (**c**) for 4 h. Data represent the means ± SEM of four independent experiments. n.s. indicates not significant and * indicates significant difference as compared to glutamate treated neurons ($p < 0.05$)

not significantly different than that of neurons incubated with glutamate (Fig. 9c and f). Both MPEP (Additional file 4: Figure S4A and Fig. 9e) and AM251 (Additional file 4: Figure S4B and Fig. 9e) eliminated CDPPB-mediated rescuing of postsynaptic sites. These data indicated that CDPPB was more efficient to protect postsynaptic terminals and that this neuroprotection was dependent on both mGluR5 and CB$_1$. JZL184 was efficient to prevent glutamate-induced decrease in syntaxin labeling (Fig. 9d and f). Moreover, JZL184 was partially efficient to avoid the loss of postsynaptic terminals, as PSD95 labeling of neurons incubated with JZL184 in the presence of

glutamate was not different than that of untreated neurons (Fig. 9d and e). However, PSD95 labeling was not different when comparing neurons incubated with glutamate in the presence or absence of JZL184 (Fig. 9d and e). AM251 eliminated the protection of both pre- and post-synaptic terminals mediated by JZL184 (Additional file 4: Figure S4D, Fig. 9e and f). Nevertheless, MPEP was only able to block JZL184-mediated rescuing of postsynaptic terminals, having no effect on syntaxin levels (Additional file 4: Figure S4C, Fig. 9e and f). These data indicated that 2-AG was more important to promote neuroprotection of presynaptic sites and that CB$_1$ and mGluR5 had

Batista *et al. Molecular Brain* (2016) 9:80
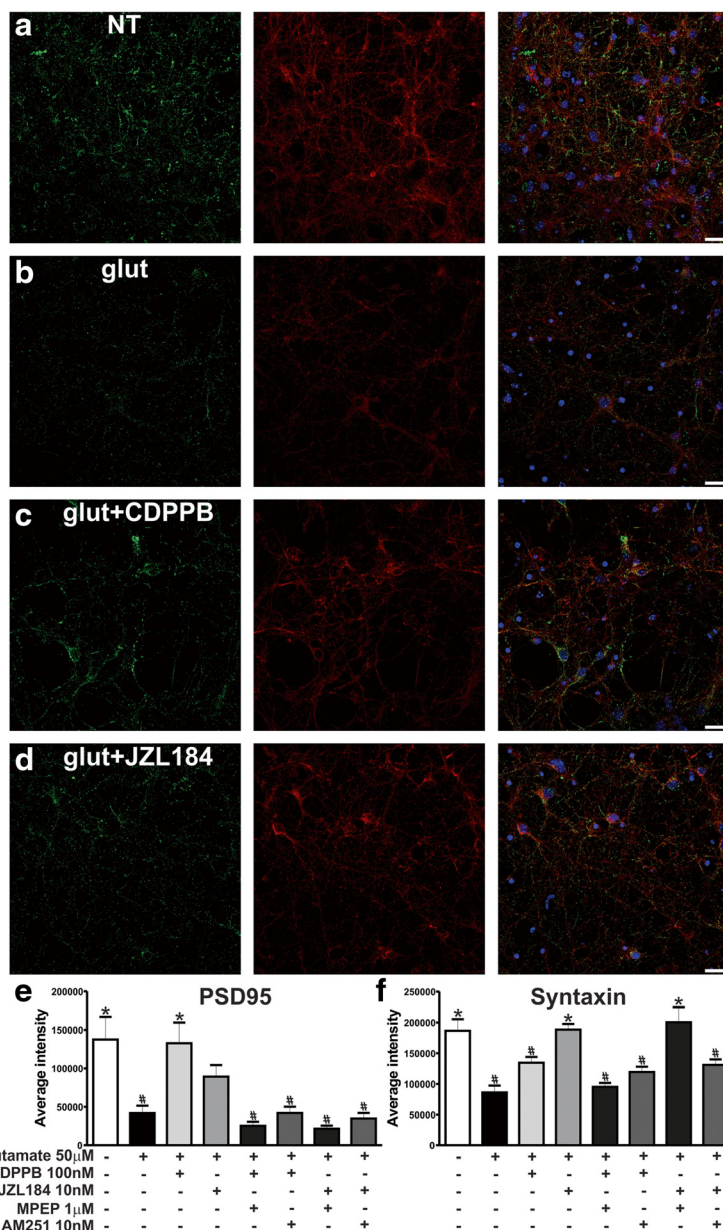
Page 12 of 17

Fig. 9 CDPPB protects postsynaptic terminals and JZL184 mainly protects the presynaptic site. Shown are laser-scanning confocal micrographs from neurons immunolabeled for PSD95 (*green*), anti-syntaxin 1A (*red*) and DAPI (*blue*), which were either untreated (NC) (**a**) or treated with 50 μM glutamate (glut) in the absence (**b**) or in the presence of 100 nM CDPPB (**c**) and 10 nM JZL184 (**d**) for 4 h. Scale bar = 20 μM. Graphs show average intensity of pixel grey levels of PSD95 (**e**) and syntaxin 1A (**f**) staining, obtained from at least five images taken from four independent experiments. Neurons were either untreated (−) or treated (+) with 50 μM glutamate, 100 nM CDPPB, 10 nM JZL184, 1 μM MPEP or 10 nM AM251, for 4 h. Data represent the means ± SEM. * indicates significant difference as compared to glutamate treated neurons and # indicates significant difference as compared to untreated neurons ($p < 0.05$)

distinct roles depending on which synaptic site was being investigated.

Discussion

Neuronal cell loss is the main feature of neurodegenerative diseases and the development of new drugs capable of preventing neuronal cell death might be an important therapeutic strategy to modify the course of these diseases. However, probably due to the complexity of the cell signaling pathways that underlie neuronal cell loss and neuroprotection of brain cells, such a disease-modifying drug is yet to be discovered [14, 55]. CB_1 and mGluR5 are promising pharmacological targets for the development of neuroprotective drugs. For instance, CB1 activation offer

Batista *et al. Molecular Brain* (2016) 9:80

Page 13 of 17

protection in various neurodegenerative diseases, including Alzheimer's disease [37, 38, 56], Parkinson's disease [30, 46], and HD [39, 41]. In the case of mGluR5, recent publications consistently indicate that mGluR5 PAMs can be neuroprotective in acute brain injury [7, 32, 68]. Moreover, our group has demonstrated that the mGluR5 PAM, CDPPB, can promote neuroprotection in vitro and that the chronic treatment of a mouse model of HD with CDPPB can prevent neuronal cell loss, decrease huntingtin aggregate formation and rescue memory deficit [10, 11].

CB_1 activation can decrease pre-synaptic release of neurotransmitters, including glutamate [44, 66]. Decreased glutamate release has been proposed as the key factor contributing to CB_1-mediated neuroprotection [28, 36]. However, CB_1-mediated neuroprotection did not involve decreased glutamate release in the present protocol. On the other hand, our data clearly shows that neuroprotection triggered by CB_1 and mGluR5 depends on both ERK1/2 and AKT activation. CB_1 and mGluR5 can activate these kinases employing different mechanisms. Stimulation of mGluRs promotes the formation of the complex mGluR-Homer-PI3K enhancer (PIKE), which allows PI3K activation by PIKE, leading to PIP3 formation, which recruits AKT and phosphoinositide-dependent kinase (PDK1) to the plasma membrane to promote AKT phosphorylation [21, 50]. Thus, activation of AKT by mGluR5 appears to be independent of $G\alpha_q$ proteins. Homer proteins are also important for mGluR5-mediated activation of ERK1/2 in the striatum and spinal cord [35, 49, 58]. Moreover, it has been shown that the proline-rich tyrosine kinase 2 (Pyk2) can be co-immunoprecipitated with both mGluR1 and mGluR5 from rat brain lysates and that Pyk2 can couple Group I mGluRs to the activation of ERK1/2 [43]. Importantly, we and others have demonstrated that mGluR5 PAMs can act as bias agonists and activate ERK1/2 and AKT, in the absence of agonist and without triggering Ca^{2+} release [5, 7, 11, 67], which was further demonstrated on this study. In the case of the cannabinoid system, it has been shown that stimulation of CB_1 can lead to activation of PI3K/AKT pathways in a mechanism that relies on $G_{\alpha io}$ proteins [15]. Moreover, ERK1/2 can be activated by CB_1 heterologously expressed in non-neuronal cell lines [4, 65]. In addition to that, it has also been demonstrated that stimulation of CB_1 can lead to ERK1/2 activation in hippocampal neurons and that PKA inhibition via uncoupling of $G\alpha_{io}$ proteins by CB_1 is important for ERK1/2 activation [8]. Importantly, activation of these cell signaling pathways by mGluR5 and CB_1 can lead to increased levels of trophic factors, including brain derived neurotrophic factor (BDNF), which has an important role in neuronal survival [2, 8, 10].

CB_1 is mostly expressed at the presynaptic site and mGluR5 at the postsynaptic region. Nevertheless these two receptors have a functional interaction, as CB_1 can regulate presynaptic glutamate release [26, 44, 66] and mGluR5 activation can increase endocannabinoid synthesis at the post-synaptic site [6, 23, 24]. However, so far it is still unclear whether mGluR5 activation could preferentially protect the post-synaptic site or whether CB_1 is more neuroprotective at the pre-synaptic area. Our data demonstrates that CDPPB offers more protection to the postsynaptic site and JZL184 protects more the presynaptic terminals. CDPPB-mediated protection of postsynaptic terminals is lost when either mGluR5 or CB_1 is blocked. Thus, it is possible that one of the mechanisms employed by mGluR5 to promote neuroprotection is to activate CB_1, which may be accomplished by increasing 2-AG synthesis following mGluR5 activation. JZL184 is very efficient to promote neuroprotection of presynaptic terminals and also offers partial rescuing of postsynaptic sites. In agreement with these data, the rescue of CB_1 expression in striatal neurons of a mouse model of HD prevents the reduction of excitatory presynaptic markers [41]. Importantly, we show in this study that MPEP is only able to block JZL184 protection of the postsynaptic terminals, but not of the presynaptic site. It is possible that the main role of mGluR5 in JZL184-mediated neuroprotection is to increase endocannabinoid synthesis, as inhibiting 2-AG degradation is not sufficient to elevate the levels of endocannabinoids to promote neuroprotection if mGluR5-mediated synthesis of 2-AG is blocked by MPEP. It has been demonstrated that disruption of the interaction between mGluR5 and DGL-α can compromise 2-AG production and long term depression (LTD) at excitatory synapses, further indicating that mGluR5 has a crucial role in 2-AG synthesis [25]. Corroborating this hypothesis, we show in this study that CB_1 direct agonists could mediate neuroprotection to some extent independently of mGluR5. However, as MPEP is still able to partially block even CB_1 direct agonist-mediated neuroprotection, it is possible that mGluR5 may have roles other than facilitate endocannabinoid synthesis to promote neuronal survival. Future experiments will be important to clarify this issue. Interestingly, mGluR5 appears to be important for JZL184-mediated neuroprotection only at the postsynaptic site, which is the main place where mGluR5-dependent 2-AG synthesis takes place. High levels of CB_1 are expressed in the presynaptic site and it is possible that low levels of endocannabinoids could be sufficient to promote neuroprotection in this case. Moreover, although JZL184 prevents the loss of presynaptic terminals independently of mGluR5, this is not enough to avoid the neuronal cell loss, as JZL184 fails to rescue neuronal cell death upon glutamate insult in the presence of MPEP. Both CB_1 and mGluR5 activate ERK1/2 and AKT and our data clearly show that this is the primary mechanism to promote neuroprotection. It has been previously demonstrated that ERK and AKT are present and can be phosphorylated/activated both in the pre- and post-synaptic terminals [3, 31, 54, 61]. Based on

Batista *et al. Molecular Brain* (2016) 9:80

Page 14 of 17

these observations, we propose that the protection of both pre- and post-synaptic sites, perhaps via activation of ERK1/2 and AKT in these two compartments, is necessary to preserve the synaptic structure and foster neuronal survival.

As summarized in "Fig. 10", we show here that activation of mGluR5 by CDPPB or CB_1 by blocking endocannabinoid degradation promotes neuroprotection against glutamate-induced excitotoxicity. Interestingly, if mGluR5 or CB_1 are blocked pharmacologically or by genetic manipulation, the
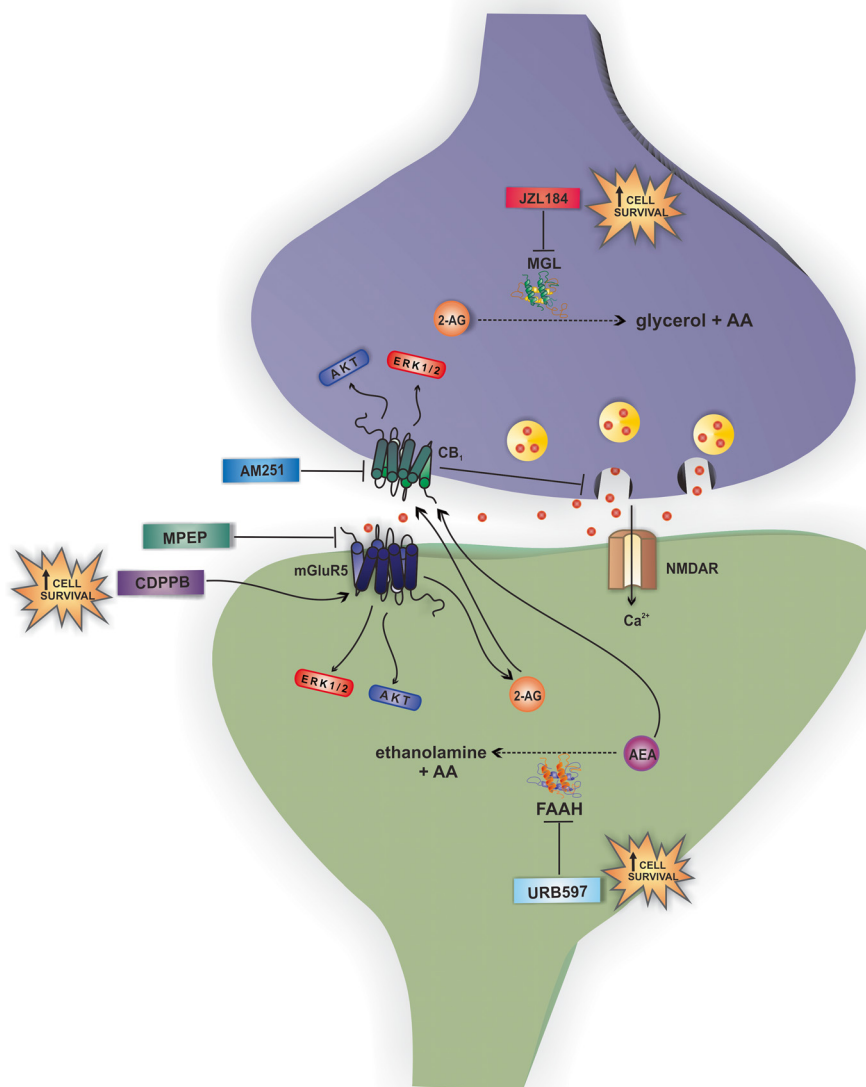
Fig. 10 mGluR5 and CB_1 cooperatively activate cell signaling pathways to promote neuroprotection. Glutamate release causes activation of N-methyl-D-aspartate receptor (NMDAR), which increases intracellular Ca^{2+}, and metabotropic glutamate receptor 5 (mGluR5), which activates various cell signaling pathways. mGluR5 is present at the postsynaptic site and can be stimulated by CDPPB, leading to the activation of different neuroprotective effectors, such as the extracellular-signal-regulated kinase 1/2 (ERK1/2) and AKT. Moreover, mGluR5 is part of a signalosome that contains the two key enzymes for 2-arachidonoylglycerol (2-AG) synthesis and, thus, mGluR5 activation can increase 2-AG levels. However, both MPEP, an mGluR5 blocker, and AM251, a CB_1 antagonist, can block mGluR5-mediated activation of ERK1/2 and AKT and, thus, neuroprotection. The cannabinoid receptor 1 (CB_1), which is present at the presynaptic site, is stimulated by 2-AG and anandamide (AEA), leading to activation of extracellular-signal-regulated kinase (ERK1/2) and AKT. CB_1 activation can also inhibit presynaptic glutamate release and, therefore, blunt mGluR5 activation by glutamate. JZL184 and URB597, which are monoacylglycerol lipase (MGL) and fatty acid amide hydrolase (FAAH) inhibitors, respectively, increase the levels of anandamide and 2-AG, leading to activation of ERK1/2 and AKT and promoting neuroprotection. However, this effect can be blocked by both MPEP and AM251. Therefore, mGluR5 and CB_1 are part of the same cell signaling pathway, working cooperatively to trigger activation of ERK1/2 and AKT and promote neuroprotection. *AA* arachidonic acid

Batista *et al. Molecular Brain* (2016) 9:80

Page 15 of 17

neuroprotection mediated by both receptors is lost, indicating that these two receptors are part of the same neuroprotective cell signaling pathway. In addition, our data demonstrate that the neuroprotection mediated by mGluR5/CB$_1$ does not rely on decreased pre-synaptic release of glutamate or decreased intracellular Ca^{2+} levels, but instead is dependent on the activation of MEK/ERK1/2 and PI3K/AKT pathways.

Additional files

Additional file 1: Figure S1. Cannabinoid receptors direct agonists can promote neuroprotection in an mGluR5-independent manner. Graph shows cell death levels of primary cultured corticostriatal neurons that were either untreated (−) or treated (+) with 50 μM glutamate, 10 nM anandamide, 10 nM 2-AG, 1 nM ACEA, 1 μM MPEP and 10 nM AM251 for 4 h. Data represent the means ± SEM of four independent experiments. * indicates significant difference as compared to glutamate treated neurons and # indicates significant difference as compared to untreated neurons (p <0.05). (TIF 270 kb)

Additional file 2: Figure S2. CB$_1$ siRNA electroporation decreases CB$_1$ protein expression. Shown are representative immunoblots for CB$_1$ (upper panel) and actin expression (lower panel) in primary cultured corticostriatal neurons that were electroporated with either NC- or CB$_1$-siRNA. Immunoblots are representative of four independent experiments. (TIF 292 kb)

Additional file 3: Figure S3. AKT activation is decreased, but not abolished, in PI3Kγ$^{−/−}$ neurons. Shown are representative immunoblots for phospho- (upper panel) and total-AKT expression (lower panel) and graphs depicting the densitometric analysis of phospho-AKT normalized to total-AKT expression in primary cultured corticostriatal neurons from PI3Kγ$^{−/−}$ embryos that were either untreated (−) or treated (+) with 50 μM glutamate, 100 nM CDPPB, 1 nM URB597 and 10 nM JZL184 for 7.5 min. 100 μg of cell lysate was used for each sample. Data represent the means ± SEM of four independent experiments. * indicates significant difference as compared to untreated neurons (p <0.05). (TIF 568 kb)

Additional file 4: Figure S4. MPEP and AM251 action on CDPPB- and JZL184-mediated protection of synaptic terminals. Shown are laser-scanning confocal micrographs depicting Alexa Fluor 488-conjugated anti-PSD95 antibody (green), Alexa Fluor 546-conjugated anti-syntaxin 1A antibody (red) and DAPI (blue) in neurons that were treated with 50 μM glutamate (glut) in the presence of 100 nM CDPPB + 1 μM MPEP (A), 100 nM CDPPB + 10 nM AM251 (B), 10 nM JZL184 + 1 μM MPEP (C) and 10 nM JZL184 + 10 nM AM251 (D) for 4 h. Scale bar = 20 μM. (TIF 8576 kb)

Availability of data and materials
The datasets supporting the conclusions of this article are included within the article and its additional files.

Authors' contributions
EMLB performed and analyzed all the experiments necessary to provide the data shown on Figs. 1, 4, 5, 6, 7 and 8 and Additional file 1: Figures S1, Additional file 2: Figures S2 and Additional file 3: Figures S3. JGD and JA performed and analyzed the experiments shown on Fig. 9 and Additional file 4: Figures S4. JGD also designed the schematic Fig. 10. THF performed and analyzed the data shown on Figs. 2 and 3. SSGF made substantial contributions to conception and design of the study and revised the manuscript critically for important intellectual content. FAM helped design the cell death experiments shown on Fig. 1 and helped writing the manuscript. FMR contributed to study conception, participated in its design and coordination and wrote the manuscript. All authors read and approved the final manuscript.

Competing interests
The authors declare that they have no competing interests.

Consent for publication
Not applicable.

Ethics approval and consent to participate
Animal care was in accordance with the Universidade Federal de Minas Gerais Ethics Committee on Animal Experimentation (CETEA) and all Animal procedures were approved by CETEA/UFMG, protocol number 3/2011.

Author details
[1]Departamento de Bioquimica e Imunologia, Instituto de Ciencias Biologicas, Universidade Federal de Minas Gerais, Ave. Antonio Carlos 6627, Belo Horizonte, MG CEP: 31270-901, Brazil. [2]Department of Cellular and Molecular Medicine, Faculty of Medicine, University of Ottawa, Ottawa K1H8M5, Canada. [3]Departamento de Farmacologia, Instituto de Ciencias Biologicas, Universidade Federal de Minas Gerais, Belo Horizonte 31270-901, Brazil.

References
1. Balschun D, Zuschratter W, Wetzel W. Allosteric enhancement of metabotropic glutamate receptor 5 function promotes spatial memory. Neuroscience. 2006;142:691–702.
2. Blazquez C, Chiarlone A, Bellocchio L, Resel E, Pruunsild P, Garcia-Rincon D, Sendtner M, Timmusk T, Lutz B, Galve-Roperh I, Guzman M. The CB1 cannabinoid receptor signals striatal neuroprotection via a PI3K/Akt/mTORC1/BDNF pathway. Cell Death Differ. 2015;22:1618–29.
3. Boggio EM, Putignano E, Sassoe-Pognetto M, Pizzorusso T, Giustetto M. Visual stimulation activates ERK in synaptic and somatic compartments of rat cortical neurons with parallel kinetics. PLoS One. 2007;2:e604.
4. Bouaboula M, Poinot-Chazel C, Bourrie B, Canat X, Calandra B, Rinaldi-Carmona M, Le Fur G, Casellas P. Activation of mitogen-activated protein kinases by stimulation of the central cannabinoid receptor CB1. Biochem J. 1995;312(Pt 2):637–41.
5. Bradley SJ, Watson JM, Challiss RA. Effects of positive allosteric modulators on single-cell oscillatory Ca2+ signaling initiated by the type 5 metabotropic glutamate receptor. Mol Pharmacol. 2009;76:1302–13.
6. Cadas H, Gaillet S, Beltramo M, Venance L, Piomelli D. Biosynthesis of an endogenous cannabinoid precursor in neurons and its control by calcium and cAMP. J Neurosci. 1996;16:3934–42.
7. Chen T, Cao L, Dong W, Luo P, Liu W, Qu Y, Fei Z. Protective effects of mGluR5 positive modulators against traumatic neuronal injury through PKC-dependent activation of MEK/ERK pathway. Neurochem Res. 2012;37:983–90.
8. Derkinderen P, Valjent E, Toutant M, Corvol JC, Enslen H, Ledent C, Trzaskos J, Caboche J, Girault JA. Regulation of extracellular signal-regulated kinase by cannabinoids in hippocampus. J Neurosci. 2003;23:2371–82.
9. Dinh TP, Carpenter D, Leslie FM, Freund TF, Katona I, Sensi SL, Kathuria S, Piomelli D. Brain monoglyceride lipase participating in endocannabinoid inactivation. Proc Natl Acad Sci U S A. 2002;99:10819–24.
10. Doria JG, de Souza JM, Andrade JN, Rodrigues HA, Guimaraes IM, Carvalho TG, Guatimosim C, Dobransky T, Ribeiro FM. The mGluR5 positive allosteric modulator, CDPPB, ameliorates pathology and phenotypic signs of a mouse model of Huntington's disease. Neurobiol Dis. 2015;73:163–73.
11. Doria JG, Silva FR, de Souza JM, Vieira LB, Carvalho TG, Reis HJ, Pereira GS, Dobransky T, Ribeiro FM. Metabotropic glutamate receptor 5 positive allosteric modulators are neuroprotective in a mouse model of Huntington's disease. Br J Pharmacol. 2013;169:909–21.
12. Fisher K, Coderre TJ. Comparison of nociceptive effects produced by intrathecal administration of mGluR agonists. Neuroreport. 1996;7:2743–7.
13. Fourgeaud L, Mato S, Bouchet D, Hemar A, Worley PF, Manzoni OJ. A single in vivo exposure to cocaine abolishes endocannabinoid-mediated long-term depression in the nucleus accumbens. J Neurosci. 2004;24:6939–45.
14. Ghezzi L, Scarpini E, Galimberti D. Disease-modifying drugs in Alzheimer's disease. Drug Des Devel Ther. 2013;7:1471–8.
15. Gomez del Pulgar T, Velasco G, Guzman M. The CB1 cannabinoid receptor is coupled to the activation of protein kinase B/Akt. Biochem J. 2000;347:369–73.
16. Grynkiewicz G, Poenie M, Tsien RY. A new generation of Ca2+ indicators with greatly improved fluorescence properties. J Biol Chem. 1985;260:3440–50.

Batista *et al. Molecular Brain* (2016) 9:80

Page 16 of 17

17. Guillermet-Guibert J, Bjorklof K, Salpekar A, Gonella C, Ramadani F, Bilancio A, Meek S, Smith AJ, Okkenhaug K, Vanhaesebroeck B. The p110beta isoform of phosphoinositide 3-kinase signals downstream of G protein-coupled receptors and is functionally redundant with p110gamma. Proc Natl Acad Sci U S A. 2008;105:8292–7.

18. Guimaraes IM, Carvalho TG, Ferguson SS, Pereira GS, Ribeiro FM. The metabotropic glutamate receptor 5 role on motor behavior involves specific neural substrates. Mol Brain. 2015;8:24.

19. Gylys KH, Fein JA, Yang F, Wiley DJ, Miller CA, Cole GM. Synaptic changes in Alzheimer's disease: increased amyloid-beta and gliosis in surviving terminals is accompanied by decreased PSD-95 fluorescence. Am J Pathol. 2004;165:1809–17.

20. Hillard CJ, Wilkison DM, Edgemond WS, Campbell WB. Characterization of the kinetics and distribution of N-arachidonylethanolamine (anandamide) hydrolysis by rat brain. Biochim Biophys Acta. 1995;1257:249–56.

21. Hou L, Klann E. Activation of the phosphoinositide 3-kinase-Akt-mammalian target of rapamycin signaling pathway is required for metabotropic glutamate receptor-dependent long-term depression. J Neurosci. 2004;24:6352–61.

22. Jew CP, Wu CS, Sun H, Zhu J, Huang JY, Yu D, Justice NJ, Lu HC. mGluR5 ablation in cortical glutamatergic neurons increases novelty-induced locomotion. PLoS One. 2013;8:e70415.

23. Jung KM, Astarita G, Zhu C, Wallace M, Mackie K, Piomelli D. A key role for diacylglycerol lipase-alpha in metabotropic glutamate receptor-dependent endocannabinoid mobilization. Mol Pharmacol. 2007;72:612–21.

24. Jung KM, Mangieri R, Stapleton C, Kim J, Fegley D, Wallace M, Mackie K, Piomelli D. Stimulation of endocannabinoid formation in brain slice cultures through activation of group I metabotropic glutamate receptors. Mol Pharmacol. 2005;68:1196–202.

25. Jung KM, Sepers M, Henstridge CM, Lassalle O, Neuhofer D, Martin H, Ginger M, Frick A, DiPatrizio NV, Mackie K, Katona I, Piomelli D, Manzoni OJ. Uncoupling of the endocannabinoid signalling complex in a mouse model of fragile X syndrome. Nat Commun. 2012;3:1080.

26. Kano M, Ohno-Shosaku T, Hashimotodani Y, Uchigashima M, Watanabe M. Endocannabinoid-mediated control of synaptic transmission. Physiol Rev. 2009;89:309–80.

27. Kathuria S, Gaetani S, Fegley D, Valino F, Duranti A, Tontini A, Mor M, Tarzia G, La Rana G, Calignano A, Giustino A, Tattoli M, Palmery M, Cuomo V, Piomelli D. Modulation of anxiety through blockade of anandamide hydrolysis. Nat Med. 2003;9:76–81.

28. Katona I, Freund TF. Endocannabinoid signaling as a synaptic circuit breaker in neurological disease. Nat Med. 2008;14:923–30.

29. Katona I, Sperlagh B, Sik A, Kafalvi A, Vizi ES, Mackie K, Freund TF. Presynaptically located CB1 cannabinoid receptors regulate GABA release from axon terminals of specific hippocampal interneurons. J Neurosci. 1999;19:4544–58.

30. Lastres-Becker I, Molina-Holgado F, Ramos JA, Mechoulam R, Fernandez-Ruiz J. Cannabinoids provide neuroprotection against 6-hydroxydopamine toxicity in vivo and in vitro: relevance to Parkinson's disease. Neurobiol Dis. 2005;19:96–107.

31. Liu M, Kay JC, Shen S, Qiao LY. Endogenous BDNF augments NMDA receptor phosphorylation in the spinal cord via PLCgamma, PKC, and PI3K/Akt pathways during colitis. J Neuroinflammation. 2015;12:151.

32. Loane DJ, Stoica BA, Tchantchou F, Kumar A, Barrett JP, Akintola T, Xue F, Conn PJ, Faden AI. Novel mGluR5 positive allosteric modulator improves functional recovery, attenuates neurodegeneration, and alters microglial polarization after experimental traumatic brain injury. Neurotherapeutics. 2014;11:857–69.

33. Long JZ, Li W, Booker L, Burston JJ, Kinsey SG, Schlosburg JE, Pavon FJ, Serrano AM, Selley DE, Parsons LH, Lichtman AH, Cravatt BF. Selective blockade of 2-arachidonoylglycerol hydrolysis produces cannabinoid behavioral effects. Nat Chem Biol. 2009;5:37–44.

34. Lu YM, Jia Z, Janus C, Henderson JT, Gerlai R, Wojtowicz JM, Roder JC. Mice lacking metabotropic glutamate receptor 5 show impaired learning and reduced CA1 long-term potentiation (LTP) but normal CA3 LTP. J Neurosci. 1997;17:5196–205.

35. Mao L, Yang L, Tang Q, Samdani S, Zhang G, Wang JQ. The scaffold protein Homer1b/c links metabotropic glutamate receptor 5 to extracellular signal-regulated protein kinase cascades in neurons. J Neurosci. 2005;25:2741–52.

36. Marsicano G, Goodenough S, Monory K, Hermann H, Eder M, Cannich A, Azad SC, Cascio MG, Gutierrez SO, van der Stelt M, Lopez-Rodriguez ML, Casanova E, Schutz G, Zieglgansberger W, Di Marzo V, Behl C, Lutz B. CB1 cannabinoid receptors and on-demand defense against excitotoxicity. Science. 2003;302:84–8.

37. Martin-Moreno AM, Brera B, Spuch C, Carro E, Garcia-Garcia L, Delgado M, Pozo MA, Innamorato NG, Cuadrado A, de Ceballos ML. Prolonged oral cannabinoid administration prevents neuroinflammation, lowers beta-amyloid levels and improves cognitive performance in Tg APP 2576 mice. J Neuroinflammation. 2012;9:8.

38. Martin-Moreno AM, Reigada D, Ramirez BG, Mechoulam R, Innamorato N, Cuadrado A, de Ceballos ML. Cannabidiol and other cannabinoids reduce microglial activation in vitro and in vivo: relevance to Alzheimer's disease. Mol Pharmacol. 2011;79:964–73.

39. Mievis S, Blum D, Ledent C. Worsening of Huntington disease phenotype in CB1 receptor knockout mice. Neurobiol Dis. 2011;42:524–9.

40. Molyneaux BJ, Arlotta P, Menezes JR, Macklis JD. Neuronal subtype specification in the cerebral cortex. Nat Rev Neurosci. 2007;8:427–37.

41. Naydenov AV, Sepers MD, Swinney K, Raymond LA, Palmiter RD, Stella N. Genetic rescue of CB1 receptors on medium spiny neurons prevents loss of excitatory striatal synapses but not motor impairment in HD mice. Neurobiol Dis. 2014;71:140–50.

42. Nicholls DG, Sihra TS, Sanchez-Prieto J. Calcium-dependent and -independent release of glutamate from synaptosomes monitored by continuous fluorometry. J Neurochem. 1987;49:50–7.

43. Nicodemo AA, Pampillo M, Ferreira LT, Dale LB, Cregan T, Ribeiro FM, Ferguson SS. Pyk2 uncouples metabotropic glutamate receptor G protein signaling but facilitates ERK1/2 activation. Mol Brain. 2010;3:4.

44. Ohno-Shosaku T, Maejima T, Kano M. Endogenous cannabinoids mediate retrograde signals from depolarized postsynaptic neurons to presynaptic terminals. Neuron. 2001;29:729–38.

45. Ohno-Shosaku T, Shosaku J, Tsubokawa H, Kano M. Cooperative endocannabinoid production by neuronal depolarization and group I metabotropic glutamate receptor activation. Eur J Neurosci. 2002;15:953–61.

46. Price DA, Martinez AA, Seillier A, Koek W, Acosta Y, Fernandez E, Strong R, Lutz B, Marsicano G, Roberts JL, Giuffrida A. WIN55,212-2, a cannabinoid receptor agonist, protects against nigrostriatal cell loss in the 1-methyl-4-phenyl-1,2,3,6-tetrahydropyridine mouse model of Parkinson's disease. Eur J Neurosci. 2009;29:2177–86.

47. Rea K, Olango WM, Harhen B, Kerr DM, Galligan R, Fitzgerald S, Moore M, Roche M, Finn DP. Evidence for a role of GABAergic and glutamatergic signalling in the basolateral amygdala in endocannabinoid-mediated fear-conditioned analgesia in rats. Pain. 2013;154:576–85.

48. Ribeiro FM, Paquet M, Ferreira LT, Cregan T, Swan P, Cregan SP, Ferguson SS. Metabotropic glutamate receptor-mediated cell signaling pathways are altered in a mouse model of Huntington's disease. J Neurosci. 2010;30:316–24.

49. Ronesi JA, Huber KM. Homer interactions are necessary for metabotropic glutamate receptor-induced long-term depression and translational activation. J Neurosci. 2008;28:543–7.

50. Rong R, Ahn JY, Huang H, Nagata E, Kalman D, Kapp JA, Tu J, Worley PF, Snyder SH, Ye K. PI3 kinase enhancer-Homer complex couples mGluRI to PI3 kinase, preventing neuronal apoptosis. Nat Neurosci. 2003;6:1153–61.

51. Russo RC, Garcia CC, Barcelos LS, Rachid MA, Guabiraba R, Roffe E, Souza AL, Sousa LP, Mirolo M, Doni A, Cassali GD, Pinho V, Locati M, Teixeira MM. Phosphoinositide 3-kinase gamma plays a critical role in bleomycin-induced pulmonary inflammation and fibrosis in mice. J Leukoc Biol. 2011;89:269–82.

52. Shen M, Piser TM, Seybold VS, Thayer SA. Cannabinoid receptor agonists inhibit glutamatergic synaptic transmission in rat hippocampal cultures. J Neurosci. 1996;16:4322–34.

53. Shigemoto R, Nomura S, Ohishi H, Sugihara H, Nakanishi S, Mizuno N. Immunohistochemical localization of a metabotropic glutamate receptor, mGluR5, in the rat brain. Neurosci Lett. 1993;163:53–7.

54. Sindreu C, Palmiter RD, Storm DR. Zinc transporter ZnT-3 regulates presynaptic Erk1/2 signaling and hippocampus-dependent memory. Proc Natl Acad Sci U S A. 2011;108:3366–70.

55. Soejitno A, Tjan A, Purwata TE. Alzheimer's disease: lessons learned from amyloidocentric clinical trials. CNS Drugs. 2015;29:487–502.

56. Stumm C, Hiebel C, Hanstein R, Purrio M, Nagel H, Conrad A, Lutz B, Behl C, Clement AB. Cannabinoid receptor 1 deficiency in a mouse model of Alzheimer's disease leads to enhanced cognitive impairment despite of a reduction in amyloid deposition. Neurobiol Aging. 2013;34:2574–84.

Batista *et al. Molecular Brain* (2016) 9:80

Page 17 of 17

57. Tang AH, Alger BE. Homer protein-metabotropic glutamate receptor binding regulates endocannabinoid signaling and affects hyperexcitability in a mouse model of fragile X syndrome. J Neurosci. 2015;35:3938–45.

58. Tappe A, Klugmann M, Luo C, Hirlinger D, Agarwal N, Benrath J, Ehrengruber MU, During MJ, Kuner R. Synaptic scaffolding protein Homer1a protects against chronic inflammatory pain. Nat Med. 2006;12:677–81.

59. Terry RD, Masliah E, Salmon DP, Butters N, DeTeresa R, Hill R, Hansen LA, Katzman R. Physical basis of cognitive alterations in Alzheimer's disease: synapse loss is the major correlate of cognitive impairment. Ann Neurol. 1991;30:572–80.

60. Ueda N, Kurahashi Y, Yamamoto S, Tokunaga T. Partial purification and characterization of the porcine brain enzyme hydrolyzing and synthesizing anandamide. J Biol Chem. 1995;270:23823–7.

61. Vara H, Onofri F, Benfenati F, Sassoe-Pognetto M, Giustetto M. ERK activation in axonal varicosities modulates presynaptic plasticity in the CA3 region of the hippocampus through synapsin I. Proc Natl Acad Sci U S A. 2009;106:9872–7.

62. Varga B, Kassai F, Gyertyan I. Interactions of CB1 and mGlu5 receptor antagonists in food intake, anxiety and memory models in rats. Pharmacol Biochem Behav. 2012;103:425–30.

63. Vilela LR, Gobira PH, Viana TG, Medeiros DC, Ferreira-Vieira TH, Doria JG, Rodrigues F, Aguiar DC, Pereira GS, Massessini AR, Ribeiro FM, de Oliveira AC, Moraes MF, Moreira FA. Enhancement of endocannabinoid signaling protects against cocaine-induced neurotoxicity. Toxicol Appl Pharmacol. 2015;286:178–87.

64. Vlahos CJ, Matter WF, Hui KY, Brown RF. A specific inhibitor of phosphatidylinositol 3-kinase, 2-(4-morpholinyl)-8-phenyl-4H-1-benzopyran-4-one (LY294002). J Biol Chem. 1994;269:5241–8.

65. Wartmann M, Campbell D, Subramanian A, Burstein SH, Davis RJ. The MAP kinase signal transduction pathway is activated by the endogenous cannabinoid anandamide. FEBS Lett. 1995;359:133–6.

66. Wilson RI, Nicoll RA. Endogenous cannabinoids mediate retrograde signalling at hippocampal synapses. Nature. 2001;410:588–92.

67. Zhang Y, Rodriguez AL, Conn PJ. Allosteric potentiators of metabotropic glutamate receptor subtype 5 have differential effects on different signaling pathways in cortical astrocytes. J Pharmacol Exp Ther. 2005;315:1212–9.

68. Zhang ZY, Sun BL, Liu JK, Yang MF, Li DW, Fang J, Zhang S, Yuan QL, Huang SL. Activation of mGluR5 attenuates microglial activation and neuronal apoptosis in early brain injury after experimental subarachnoid hemorrhage in rats. Neurochem Res. 2015;40:1121–32.